Year: 2012

Adeno-associated virus type 2 modulates the host DNA damage response induced by herpes simplex virus type 1 during co-infection

Vogel, R ; Seyffert, M ; Strasser, R ; de Oliveira, A P ; Dresch, C ; Glauser, D L ; Jolinon, N ; Salvetti, A ; Weitzman, M D ; Fraefel, C ; Ackermann, M

DOI: https://doi.org/10.1128/JVI.05694-11

Originally published at:
Vogel, R; Seyffert, M; Strasser, R; de Oliveira, A P; Dresch, C; Glauser, D L; Jolinon, N; Salvetti, A; Weitzman, M D; Fraefel, C; Ackermann, M (2012). Adeno-associated virus type 2 modulates the host DNA damage response induced by herpes simplex virus type 1 during co-infection. Journal of Virology, 86(1):143-155.
DOI: https://doi.org/10.1128/JVI.05694-11

JVI Accepts, published online ahead of print on 19 October 2011
J. Virol. doi:10.1128/JVI.05694-11

Adeno-associated virus type 2 modulates the host DNA damage response induced by herpes simplex virus type 1 during co-infection.

Rebecca Vogel,[1] Michael Seyffert,[1] Regina Strasser,[1] Anna P. de Oliveira,[1] Christiane Dresch,[1] Daniel L. Glauser,[2] Nelly Jolinon,[3] Anna Salvetti,[3] Matthew D. Weitzman,[4†] Mathias Ackermann,[1] , and Cornel Fraefel[1]*

[1]Institute of Virology, University of Zurich, Zurich, Switzerland. [2]Division of Virology, Department of Pathology, University of Cambridge, Cambridge, United Kingdom. [3]INSERM U758, Ecole Normale Supérieure de Lyon, Lyon, France. [4]The Salk Institute for Biological Studies, La Jolla, CA, USA.

† Present address: Center for Cellular and Molecular Therapeutics, The Children's Hospital of Philadelphia, PA, USA.

*Corresponding author. Mailing address: Institute of Virology, University of Zurich, Winterthurerstrasse 266a, 8057 Zurich, Switzerland. Phone: +41 44 6358713, Fax: +41 44 6358911, E-mail: cornel.fraefel@access.uzh.ch

Running title: HSV-1-supported AAV2 replication-induced DDR

Word count abstract:180
Word count text: 5616

Abstract

Adeno-associated virus type 2 (AAV2) is a human parvovirus that relies on a helper virus for efficient replication. Herpes simplex virus type 1 (HSV-1) supplies helper functions and changes the environment of the cell to promote AAV2 replication. In this study, we examined the accumulation of cellular replication and repair proteins at viral replication compartments (RCs) and the influence of replicating AAV2 on HSV-1 induced DNA damage responses (DDR). We observed that the ATM kinase was activated in cells co-infected with AAV2 and HSV-1. We also found that phosphorylated ATR kinase and its cofactor ATR interacting protein (ATRIP) were recruited into AAV2 RCs, but ATR signaling was not activated. DNA-PKcs, another main kinase in the DDR, was degraded during HSV-1 infection in an ICP0-dependent manner, and this degradation was markedly delayed during AAV2 co-infection. Furthermore, we detected phosphorylation of DNA-PKcs during AAV2 but not HSV-1 replication. The AAV2-mediated delay in DNA-PKcs degradation affected signaling through downstream substrates. Overall, our results demonstrate that co-infection with HSV-1 and AAV2 provokes a cellular DDR which is distinct from that induced by HSV-1 alone.

Introduction

Adeno-associated virus type 2 (AAV2) is a small, non-enveloped parvovirus with a single-stranded DNA genome of 4.7 kb (52). In absence of a helper virus, AAV2 establishes a latent infection, which is characterized by site-specific integration of the viral genome into the AAVS1 site on human chromosome 19 (72). In presence of a helper virus, AAV2 can replicate productively in the host cell nucleus. AAV2 DNA replication occurs at discrete sites in the nucleus, termed replication compartments (RCs). During the course of infection, several small RCs rapidly expand and fuse to large structures, which displace the cellular chromatin and fill the entire cell nucleus (28, 35, 37, 79, 91). AAV2 RCs contain AAV2 proteins as well as defined helper virus proteins and cellular proteins (3, 35, 63, 65, 75, 79, 90, 91). Replicating AAV2 has inhibitory effects on both the host cell (9, 41, 68, 71, 73, 74, 100, 101) and the helper virus (5, 30, 31, 34, 40, 44, 61, 84, 100).

One of the helper viruses for AAV2 replication is herpes simplex virus type 1 (HSV-1; (14)). The minimal HSV-1 helper factors for AAV2 replication from plasmid substrates include the helicase-primase complex encoded by UL5, UL8, and UL52, and the major DNA binding protein ICP8 (3) (90). Besides viral helper factors, the fate of AAV2 replication also depends on cellular proteins. Recently, cellular proteins have been identified that interact with AAV2 Rep78/68 in adenovirus (Ad) or HSV-1 supported AAV2 replication (63, 65). Of these, the largest functional categories correspond to cellular proteins which are involved in DNA metabolism including DNA replication, repair, and chromatin modification.

There is accumulating evidence that the DNA damage response (DDR) pathways play central roles in viral replication (92). Controlling the DDR signaling may be a mechanism to prevent apoptosis and/or stop cell cycle progression (92). For example DNA damage signaling has been shown to enhance the replication of autonomous parvovirus minute virus of mice (MMV), perhaps in part by promoting cell cycle arrest (1). In response to DNA damage, a complex signaling network is activated that includes kinase regulation, transcriptional induction, and redistribution of a multitude of factors (33, 38). Depending on the extent of DNA damage, cell cycle progression is stopped to repair DNA breaks or apoptosis is induced. Two main pathways are classified for the repair of DNA double-strand breaks, homologous recombination and non-homologous end-joining (16, 36, 99). Proteins which are important for sensing DNA double-strand breaks include H2AX and the Mre11/Rad50/Nbs1 (MRN) complex (for a review see (47)). The phosphatidylinositol-3-kinase-like kinases (PIKKs) Ataxia Telangiectasia mutated (ATM) and ATM and Rad3 related (ATR) are proximal signaling kinases that have key functions in signaling transduction in homologous recombination (24, 33, 60, 66, 69). ATM is recruited by the MRN complex (for a review see (29)) and catalytically activated through dimer dissociation and auto-phosphorylation at serine (S) 1981 (6, 103). Examination of ATR recruitment to sites of DNA damage revealed that binding of ATR to ATRIP leads to co-localization of the ATR-ATRIP complex with replication protein A (RPA)-coated single-stranded DNA (7). It is suggested that interaction of topoisomerase II-binding protein 1 with the ATR-ATRIP complex induces kinase activity of ATR (59). A third PIKKs, DNA-dependent protein kinase (DNA-PK) belongs to the non-homologous end-joining machinery and is composed of the Ku70/Ku80 hetero-dimer and the catalytic subunit of DNA-PK (DNA-PKcs). Ku70/80 directly recognizes DNA double-strand breaks and activates DNA-PKcs (for a review see (15)). Activity of DNA-PKcs is proposed to be regulated by autophosphorylation at several sites, including S2056 (19, 21). Investigation of downstream signaling via PIKKs suggests that checkpoint kinase (Chk) 1 is mainly a substrate of ATR after recognition of single-strand breaks and stalled-replication forks (22, 32, 53, 80, 83, 105), while Chk2 activation by ATM is more restricted to double-strand breaks, including those induced by ionizing radiation (IR) (2, 20, 42, 43, 56, 57). However, there is evidence that ATR (85, 87) and DNA-PK (50, 85) can also induce Chk2 phosphorylation. DNA-PK (49, 86, 88), ATR (46), and ATM (8) have all been reported to induce phosphorylation of p53.

HSV-1 induces activation of a cellular DNA double-strand break response pathway involving the MRN complex, ATM, p53, RPA (non-phosphorylated), and Rad51 (13, 51, 76, 96), while the ATR response has been reported to be inhibited (58, 94). Similarly, signaling via DNA-PK is also inhibited by HSV-1 through ICP0-dependent proteasomal degradation of DNA-PKcs (48, 67). It has been shown that in absence of the Ku70 subunit of the DNA-PK complex, HSV-1 replication is enhanced (81). AAV2, although not replicating in absence of a helpervirus, induces a strong DDR mediated by ATR (41). A different DDR is induced upon co-infection with a helpervirus that supports AAV2 replication; for example, during Ad supported AAV2 replication, the DDR signaling is primarily mediated by DNA-PK and is independent of the MRN complex (25, 75). Furthermore, activation of ATM, Chk1, Chk2, RPA, and H2AX was also observed (25, 75). Given that DNA-PK is a key kinase in non-homologous end-joining, it seems that these events may play important roles not only in (site-specific) integration of the AAV2 genome (18, 27, 77), but also in AAV2 genome replication (23). As opposed to Ad and AAV2 co-infection, the DDR induced by co-infection with HSV-1 and AAV2 have not previously been investigated. Thus, the goal of the present study was to identify cellular replication and repair proteins that accumulate at AAV2 RCs when HSV-1 is the helper virus, and to determine the effect of AAV2 on the cellular DDR signaling pathways induced by HSV-1.

Materials and Methods

Cells. DNA-PKcs positive (expressing one copy of DNA-PKcs) and DNA-PKcs negative HCT116 cells were kindly provided by E. Hendrickson (University of Minnesota Medical School, Minneapolis, USA) and maintained in growth medium containing Dulbecco's modified Eagle medium (DMEM) supplemented with 10% fetal bovine serum (FBS), 100 units/ml penicillin G, 100 µg/ml streptomycin, and 0.25 µg/ml amphotericin B (1% AB). DNA-PKcs positive (Fus1) and DNA-PKcs negative (Fus9) MO59J cells were kindly provided by T. Melendy (Department of Cellular and Molecular Biology, Roswell Park Cancer Institute, Buffalo, USA.) and cultured in 50% F10 medium/50% DMEM supplemented with 10% FBS, 1% AB, and 250 µg/ml G418. The fibroblast cells AT22 IJE-T yZ5 (expressing ATM) and AT22 IJE-T pEBS7 (lacking ATM) were kind gifts from Y. Shiloh (Department of Molecular Genetics and Biochemistry, Sackler School of Medicine, Tel Aviv University, Tel Aviv, Israel). These cells were maintained in DMEM supplemented with 10% FBS, 1% AB and 100 µg/ml Hygromycin B. U2OS GW33 cells were a kind gift from P. Nghiem (Department of Medicine/Dermatology, University of Washington, Seattle, USA) and were cultured in DMEM containing 10% FBS, 1% AB, 200 µg/ml G418 and 50 µg/ml Hygromycin B. Vero cells were maintained in DMEM supplemented with 10% FBS, 1% AB. All cells were maintained at 37°C in a 95% air/5% CO_2 atmosphere.

Viruses. HSV-1 strain F was kindly provided by B. Roizman (Marjorie B. Kovler Viral Oncology Laboratories, University of Chicago, Chicago, USA). rHSV-1 dl1403 (rHSV-1∆ICP0) was kindly provided by N.D. Stow (MRC Virology Unit, University of Glasgow, Glasgow, United Kingdom), and rHSV-1vEYFP-ICP4 and rHSV-1 vECFP-ICP4 was a kind gift R.D. Everett (MRC Virology Unit, University of Glasgow, Glasgow, United Kingdom). Viruses were grown on Vero cells. HSV-1 stain F was titrated on Vero cells and rHSV-1 dl1403 was titrated on U2OS cells. AAV2 and Ad2 were kindly provided by H. Buening (University of Cologne, Cologne, Germany) and U. Greber (University of Zurich, Zurich, Switzerland), respectively. Recombinant AAV2CherryRep (rAAVCR) genomes, containing the AAV2 ITR flanking the *rep* ORFs fused at its 5' terminus with the mCherry coding sequence, has been described previously (3). Recombinant AAVCR particles of AAV serotype 2 were produced by transient transfection of 29356 with pDG and pAAVCR, purified on two successive CsCl gradients and genome containing particles titered by Dot Blot. rAAV2GFP was kindly provided by M. Linden (King's College London School of Medicine, London, UK).

Antibodies. The following primary antibodies were used: Anti-actin (Santa Cruz Biotechnology (SC) 10731; dilution WB 1:10'000), anti-ATM (Genetex 70107; dilution WB: 1:1000), anti-ATM-P-S1981 (Rockland Immunochemicals (RI) 200-301-400; dilution WB 1:500, IF 1:50), anti-ATR (SC-28901, dilution WB 1:1000), anti-ATR-P-S428 (Cell Signaling Technology (CST) 2853, dilution WB 1:500, IF 1:200), anti-ATRIP (Abcam (Ab) 19531; dilution WB 1:2000, IF 1:500), anti-Chk1 (SC 8408; dilution WB 1:1000), anti-Chk1-P-S345 (CST 133D3, dilution WB 1:1000), anti-Chk2 (SC 5278; dilution WB: 1:1000), anti-Chk2-P-T68 (SC 16297; dilution WB/IP 1:250, IF 1:100), anti-DNA-PKcs (NeoMarkers M5370; dilution WB 1:500, IF 1:50, Flow cytometry 1:250), anti-DNA-PKcs-P-S2056 (Ab 18192; dilution WB 1:2000, IF 1:500), anti-HSV-1 ICP8 (Ab 20193; dilution WB 1:1000, IF 1:200), anti-H2AX-P-S139 (Millipore 05-636; dilution WB 1:500, IF 1:50), anti-Nbs1 (Novus Biologicals 100-143; dilution WB 1:1000), anti-Nbs1-P-S343 (Ab 47272; dilution WB 1:500, IF 1:100), anti-p53 (Ab 1101; dilution WB: 1:1000), anti-p53-P-S15 (Ab 38497 (Antibody was purchased in June 2009, is not available anymore); dilution WB 1:500, IF 1:500), anti-AAV2 Rep (Fitzgerald Industries 10R-A111A; dilution WB 1:200), anti-RPA32 (Bethyl Laberatories (BL) A300-244A; dilution WB 1:2000, IF 1:500), anti-RPA32-P-S4/8 (BL A300-245A; dilution WB 1:200, IF 1:200); anti-USP7 (CST 3277; dilution WB 1:750). The following secondary antibodies were used: Rabbit anti-mouse IgG-horseradish peroxidase (HRP, Sigma A9044; dilution 1:10000), goat anti-rabbit IgG-HRP (Sigma A6154; dilution 1:10000), rabbit TrueBlot®, goat anti-rabbit IgG (H+L)-AlexaFlour(AF)405 (Molecular Probes A31556; dilution 1:500), goat anti-rabbit IgG (H+L)-AF594 (Molecular Probes A11012; dilution 1:1000), goat anti-mouse IgG (H+L)-AF594 (Molecular Probes A11005; dilution 1:1000), goat anti-mouse IgG (H+L)-fluorescein isothiocyanate (FITC, Southern Biotechnology 1031-02; dilution 1:200), goat anti-rabbit IgG (H+L)-FITC (Southern Biotechnology 4050-02; dilution 1:200), goat anti-mouse IgG-Cy5 (Millipore AP181S; dilution 1:500).

Western analysis. 10^6 HCT116 cells, $5x10^6$ AT22 IJE-T, or $5x10^6$ MO59J fusion cells were seeded into 6cm plates. The following day, the cells were mock-infected, infected with either AAV2 (multiplicity of infection, MOI, 2000) or HSV-1 (MOI 1.5), or co-infected with AAV2 (MOI 2000) and HSV-1 (MOI 1.5) in DMEM supplemented with 2% FBS and 1% AB. Cells treated for 18 h with hydroxyurea (3 mM) served as positive control for activation of DDR proteins. After 3h, 6h, 9h, 12 h, 24 h, or 48 h, cells were trypsinized, washed once with PBS and resuspended in 200 µl EBC-170 lysis buffer (50 mM Tris-HCL, 170 mM NaCl, 0.5% Nonidet P40, protease inhibitor (Complete Mini-EDTA-free, Roche Diagnostics, Rotkreuz, Switzerland). After 30 min of incubation at 4°C under constant agitation, the suspension was centrifuged (20 min at 13'200 g), the supernatant collected, mixed with 2x loading buffer (4% SDS, 10% β-mercaptoethanol, 20% glycerol, 0.005% bromphenol blue, 0.125 M Tris-HCL, pH 6.8) and boiled for 10 min. Cell lysates were separated, depending on the molecular weight of the protein of interest on 8%, 10%, or 12% SDS polyacrylamide-gels and transferred to Protran nitrocellulose membranes (Protan, Whatman, Bottmingen, Switzerland). For detection of γH2AX, proteins were separated on a 12% SDS polyacrylamide-gel and transferred to a PVDF membrane with a pore size of 0.45 µm (Amersham Hybond™-P GE Healthcare Bio-Sciences AB, Uppsala Sweden). The membranes were blocked with PBS-T (PBS containing 0.3% Tween20) supplemented with 5% non-fat dry milk for 1 h at room temperature (RT). Incubation with antibodies was carried out in PBS-T supplemented with 2.5% non-fat dry milk. Primary antibodies were incubated over night at 4°C, while secondary antibodies were incubated for 1 h at RT. Membranes were washed three times with PBS-T for 10 min after each antibody incubation step. HRP-conjugated secondary antibodies were detected with ECL detection reagent (ECL Western blotting analysis systems; GE Healthcare, Zurich, Switzerland). The membranes were exposed to chemiluminescent detection films (Roche Diagnostics, Rotkreuz, Switzerland). Detection of â-actin served as loading control of the lysate.

Fluorescence-activated cell sorting (FACS) and Western anaylsis. $6.6x10^6$ AT22IJE-T cells were seeded into 10 cm cell culture dishes. Cells were mock-infected, infected with rHSV-1vECFP-ICP4 (MOI 2 or 4), or co-infected with rHSV-1vECFP-ICP4 (MOI 2 or 4) and rAAV2CR (MOI 4000). Cells positive for mCherry (rAAV2) or ICP4-ECFP (HSV-1) were sorted and prepared for Western analysis as described above. The same number of mock-infected and HU treated cells (3mM, 18hpi) were used as controls.

Immunoprecipitation. AT22 IJE-T cells (90'000) were seeded into 6-well plates. The next day, cells were mock-infected, infected with either AAV2 (MOI 2000) or HSV-1 (MOI 1.5), or co-infected with AAV2 (MOI 2000) and HSV-1 (MOI 1.5) in DMEM supplemented with 2% FBS and 1% AB. After 24 h, cells were trypsinized, washed once with PBS, and resuspended in 200 µl EBC-170 lysis buffer containing the primary antibody. After incubation for 2 h at 4°C under constant agitation, 30 µl Protein A Sepharose CL-4B (GE Healthcare, Zurich, Switzerland) were added and incubated for 2 h at 4°C under constant agitation. Then, sepharose beads were pelleted and the supernatant was collected as loading and infection controls. The pellet was washed twice with PBS for 15 min at 4°C under constant agitation, and protein was eluted using 20-40 µl of a 4 M urea solution (pH 7.5). After 10 min incubation at 4°C under constant agitation, beads were pelleted, and the supernatant was collected. Samples were analyzed by Western blotting as described above; however, for detection of immunoprecipitated proteins, the secondary antibody rabbit IgG TrueBlot® (Anti-Rabbit IgG HRP, eBioscience, San Diego, CA, USA) was used, which preferentially detects the non-reduced form of rabbit IgG over the reduced, SDS-denatured form of IgG.

Immunofluorescence analysis. HCT116 cells (5x10^4), AT22 IJE-T cells (7,5x10^4), or MO59J fusion cells (7,5x10^4) were seeded onto cover slips (12 mm ø, Glaswarenfabrik Karl Hecht GmbH&Co KG, Sondheim, Germany) in 24-well plates. The next day, cells were mock-infected, infected with HSV-1 (MOI 1.5), or co-infected with rAAV2CR (MOI 250) and either HSV-1 (MOI 1.5), rHSV-1dl1403 (MOI 0.9) or Ad2 (MOI 12). UV-exposed cells (10 J/m^2) or hydroxyurea (HU, 3mM) treated cells served as positive control for activation of DDR proteins. After 24 h, cells were washed once with cold PBS and fixed with 3.7% formaldehyde in PBS for 15 min at RT. The fixation process was stopped with 0.1 M glycine for 10 min at RT. Cells were washed twice with cold PBS. For permeabilization, cells were treated for 2 min with pre-cooled acetone (-20°C) and washed three times with PBS. Cells were blocked for 30 min with 3% BSA in PBS. For staining, cells were incubated with antibodies diluted in PBS-BSA (3%) in a humidified chamber at RT in the dark. Cover slips were placed on droplets (40 µl) of primary antibody solution. After incubation for 1 h, cells were washed three times with PBS. DAPI (4',6' diamidino-2-phenylindole) staining was performed together with the secondary antibody staining. For this, DAPI (0.5 µg/ml) and the secondary antibody were diluted in PBS-BSA (3%). After incubation for 1h at RT in the dark, cells were washed three times with PBS and once with H_2O. Cover slips were embedded in Glycergel (DakoCytomation, Carpinteria, USA) containing DABCO (26 mg/ml, Fluka, Sigma-Aldrich Chemie Gmbh, Munich, Germany), and cells were observed using a confocal laser scanning microscope (CLSM, Leica TCS SP2 AOBS, Leica Mycrosystems, Wetzlar, Germany). To prevent crosstalk between the channels for the different fluorochromes, all channels were recorded separately and fluorochromes with longer wavelengths were recorded first. Images from CLSM were deconvolved with Huygenes Essential 2.6.0p1 software (Scientific Volume Imaging, Hilversum, Netherlands) and processed using Imaris 5.0.1 (Bitplane AG, Zurich, Switzerland).

Flow cytometry. The day before infection, 10^6 HCT116 cells were seeded into 6 cm tissue culture plates. The cells were mock-infected, infected with rHSV-1vEYFP-ICP4 (MOI 1.5), or co-infected with AAV2 (MOI 250), rAAV2GFP (MOI 250), and HSV-1 (MOI 1.5) in DMEM supplemented with 2% FCS and 1% AB, and incubated for 20 h at 37°C in a 5%CO_2 atmosphere. Cells were trypsinized and washed once with PBS. For fixation and staining, the BD Cytofix/Cytoperm™ Plus Kit (BD Biosiences) was used according to the manufacturer's instructions. Flow cytometry was performed on a FACScalibur (Becton-Dickinson). DNA-PKcs-contents were analyzed in HSV-1-infected cells positive for EYFP-ICP4 (rHSV-1 encoded) and in co-infected cells positive for EGFP (rAAV encoded). A minimum of 80`0000 events were scored for each sample. The mean fluorescence intensity (MFI) of cell-populations was determined using Flowjo software (Flowjo Version 8.6.3, Stanford University, Stanford, CA, USA).

Results

Activation of primary DNA damage markers Nbs1 and H2AX upon virus infection. We compared the DDR of cells infected with HSV-1 alone or co-infected with AAV2. As we have previously observed that at low MOI, HSV-1 supported AAV2 RCs are not detectable before approximately 18 hpi, we analyzed the cells for up to 48 hpi.

The overall levels of Nbs1 were not altered by virus infection (Fig. 1A). However, Nbs1 was phosphorylated upon infection with HSV-1 alone or co-infection with AAV2 (Fig. 1B); moreover, phosphorylated Nbs1-P-S343 co-localized with AAV2 RCs and with HSV-1 RCs (Fig. 2A). Nbs1 expression was also examined in AT22 IJE-T and HCT116 cells with similar results (data not shown). In HCT116 cells, HSV-1 and co-infection induced phosphorylation was also indicated by shifted Nbs1 bands (data not shown). In addition, H2AX was found to be phosphorylated (Fig. 1A) and to surround HSV-1 supported AAV2 RCs (Fig. 2B). As previously observed H2AX also surrounded HSV-1 RCs (Fig. 2B (94)).

Co-infection with AAV2 and HSV-1 induces the phosphorylation of ATM and ATR. Previous studies revealed that ATM-mediated signaling is induced (51, 76, 96) and that ATR-mediated signaling is blocked in HSV-1 infected cells (58, 94). To examine the activity of these two PIKKs in cells co-infected with HSV-1 and AAV2, we first determined their phosphorylation status by Western blot and immunofluorescence analysis. While total ATM levels were similar in virus-infected cells and mock-infected cells (Fig. 1A), ATM-dependent staining with an antibody generated to auto-phosphorylated ATM was detected only in cells infected with HSV-1 alone or co-infected with AAV2 (Fig. 1B) and, in these cells, co-localized with HSV-1 and AAV2 RCs (Fig. 3A). As this antibody detects other phosphorylated targets of ATM such as 53BP1, this data only demonstrates that the staining requires ATM activity but does not necessarily represent ATM itself.

Total ATR levels were also comparable in virus–infected cells and mock-infected cells (Fig. 1A), but phosphorylated ATR-P-S428 was present only in cells infected with either HSV-1 or AAV2 alone or co-infected with both viruses (Fig. 1A), and it co-localized with approximately 85% of HSV-1 RCs and approximately 87% of AAV2 RCs (Fig. 3B). The observed phosphorylation of ATR in cells infected with HSV-1 alone was surprising, as it appeared to be in contrast to previous studies which did not find HSV-1-induced activation of ATR (58, 94). We therefore further investigated the phosphorylation/activation of ATR by: (i) testing the specificity of the ATR-P-S428 antibody (70) (ii) monitoring ATRIP, a protein that is important for the recruitment of ATR to sites of DNA damage (89, 106) and (iii) analyzing the phosphorylation status of the ATR target Chk1. The results of these experiments can be summarized as follows: (i) Immunoprecipitation with an ATR specific antibody resulted in ATR-P-S428 specific bands in cells infected with HSV-1 and/or AAV2, but not in mock-infected cells (Fig. S1A). (ii) ATRIP was detected both in mock-infected cells and virus-infected cells (Fig. 1A), where it co-localized with AAV2 and HSV-1 RCs (Fig. 3C). (iii) Western analysis revealed no phosphorylation of the ATR target Chk1 at S345 (Fig S1B) and S317 (data not shown) in infected cells. Concluding from the results above, it seems that although ATR is phosphorylated in infected cells, the kinase is not activated and therefore not able to transmit DDR signaling via its downstream target Chk1. Supporting this, Nam et al. (62) recently showed that phosphorylation of ATR on S428 is not indicative of ATR activity and cannot be inhibited by the commonly used ATR inhibitor caffeine. Moreover, Liu et al. reported that the mutation of S428 to A428 did not prevent phosphorylation of Chk1 in response to replicative stress (54).

HSV-1 ICP0 dependent degradation of DNA-PKcs is delayed during co-infection with AAV2. HSV-1 ICP0 is known to induce proteasomal degradation of DNA-PKcs (48, 67), which together with Ku70 and Ku80 forms DNA-PK, the third main PIKK besides ATM and ATR (reviewed in (55)). Consistent with these reports, our Western blot results displayed loss of DNA-PKcs by 48 h after infection with HSV-1 or co-infection with HSV-1 and AAV2 (Fig. 1A). Accordingly, at the single cell level, DNA-PKcs was not detected simultaneously with either the HSV-1 immediate-early protein ICP0 or the HSV-1 early protein ICP8 in cells infected with HSV-1 alone. However, DNA-PKcs was readily detected in cells infected with rHSV-1ΔICP0 (Fig. 4A). Interestingly, immunofluorescence analysis revealed that DNA-PKcs co-localized with the HSV-1 proteins ICP0 and ICP8 in 80% and 76% of AAVRCs, respectively (Fig. 4B). This indicates that HSV-1 ICP0-mediated DNA-PKcs degradation in co-infected cells is not as efficient as in the cells that are infected with HSV-1 alone, even if intensity of DNA-PKcs staining in large AAV RCs is decreased compared to small AAV RCs (Fig. 4B). This possibility was further investigated by flow cytometry data. Cells infected with HSV-1 or co-infected with HSV-1 and AAV2 were identified using rHSV-1 and rAAV expressing ICP4-EYFP or EGFP, respectively. Similar to the results obtained with wtHSV-1 (strain F), DNA-PKcs was degraded also in cells infected with the autofluorescent recombinant HSV-1 (strain17; Fig. 4C). By contrast, the fluorescence intensity of DNA-PKcs staining in cells co-infected with wtHSV-1 and AAV2 was at the same level as that in mock-infected cells (Fig. 4C). At the chosen MOIs, the ratio of cells that show AAV RCs at 24 hpi is only approximately 10%, while 24 h after infection with HSV-1 alone, more than 40% of the cells contain HSV-1 RCs. This may explain why in the Western analysis of total cell lysates shown in Figure 1, the degradation of DNA-PKcs appeared equally efficient in HSV-1 infected cells and in co-infected cells, while on the single cell level (Fig. 4, B and C) DNA-PKcs degradation appeared to be less efficient in co-infected cells.

To further examine this observation, we performed Western analysis of sorted cells at 22 and 26 hpi (Fig. 4D and E). For this, cells were infected with rHSV-1 ICP4-ECFP or co-infected with rAAVCR and rHSV-1 ICP4-ECFP. HSV-1 infected cells were sorted based on the expression of ICP4-ECFP and cells that contain replicating rAAV RCs were sorted based on the expression of mCherry-Rep. Sorted mock-infected cells served as control. Mock-infected and HU treated cells served as activation control for DNA-PKcs. Quantification of the Western blot shown in Fig. 4 D, revealed 3-times higher levels of DNA-PKcs at 22 hpi during AAV replication as compared to cells infected with HSV-1 alone (Fig. 4D). At 26 hpi, the intensity of the DNA-PKcs staining was also decreased in co-infected cells compared to 22 hpi, but still approximately 2-times higher than in cells infected with HSV-1 alone at 26 hpi. Moreover, phosphorylation of DNA-PKcs at S2056 was detected only in cells co-infected with both viruses (Fig. 4, E and F), however pDNA-PKcs-levels decreased also in co-infected cells over time (Fig. 4E). Staining for cellular deubiquitinase ubiquitin specific peptidase 7 (USP7) at 24 hpi, which is another known target of

HSV-1 ICP0-induced proteasomal degradation (12), revealed that the AAV-mediated delay of the ICP0 function was specific for DNA-PKcs, as the degradation of USP7 was equally efficient in cells infected with HSV-1 alone and in co-infected cells (Fig. 4F).

Next, we analyzed the localization of DNA-PKcs-P-S2056 within infected cells. As positive and negative controls we co-infected DNA-PKcs-positive cells and DNA-PKcs-deficient cells with Ad and AAV2 which are known to activate and recruit DNA-PKcs into RCs (75). While DNA-PKcs-P-S2056 staining was readily detected in cells co-infected with AAV2 and either Ad2 or HSV-1, where it also co-localized with AAV2 RCs, we did not observe staining in cells that contained HSV-1 RCs (Fig. 4G).

Phosphorylation of Chk2 and p53. To explore a potential DNA-PK-mediated signaling to downstream targets in co-infected cells, we assessed virus induced phosphorylation of Chk2 and p53 in normal cells and in cells defective for either DNA-PKcs (MO59J Fus9) or ATM (AT22 IJE-T pEBS7). HSV-1 has previously been shown to induce the phosphorylation of Chk2 in an ATM-dependent manner (51, 76). Our results are in line with these reports as in normal cells (data not shown) and in DNA-PKcs-deficient cells (Fig. 5A), Chk2 was phosphorylated at 24 h after infection with HSV-1, and this occurred also in cells co-infected with HSV-1 and AAV2. However, in ATM-deficient cells, Chk2 was phosphorylated only in cells co-infected with both viruses but not in cells infected with HSV-1 alone (Fig. 5, B). This suggests that in these cells, Chk2 phosphorylation was possibly facilitated by the AAV2-mediated delayed degradation of DNA-PKcs. Also consistent with previous observations, we detected that HSV-1 (13) and AAV2 (68) induced the stabilization of p53 (Fig. 1C). Additionally, we observed that p53 was phosphorylated at S15 in cells infected with either HSV-1 or AAV2, or co-infected with both viruses (Fig. 1C), and p53-P-S15 was recruited into both HSV-1 RCs and AAV2 RCs (data not shown). p53-P-S15 was also detected in DNA-PKcs-deficient cells infected with HSV-1 alone or co-infected with HSV-1 and AAV2 (Fig. 5A); in these cells phosphorylation is likely ATM-mediated. However, as opposed to the situation in normal cells infected with AAV2 alone, p53-P-S15 was not detected in DNA-PKcs-deficient cells infected with

AAV2 alone (Fig. 5A), indicating that in absence of the helpervirus, AAV2 induced phosphorylation of p53 is DNA-PK-dependent. In ATM-deficient cells, p53 was phosphorylated only when cells were infected with rHSV-1ΔICP0 or co-infected with AAV2 and HSV-1 (Fig. 5C), but not in cells infected with HSV-1 alone (Fig. 5C), indicating again that in co-infected cells p53 phosphorylation was supported by the delayed degradation of DNA-PKcs.

Phosphorylation of RPA. The trimeric RPA complex composed of RPA70, RPA32, and RPA14 is involved in DNA repair as well as replication and transcriptional regulation of both cellular and viral DNA (10, 97). RPA has a strong affinity to single-stranded DNA (98) and was shown to be a component of Ad supported AAV2 RCs (79). Upon DNA damage, RPA32 becomes phosphorylated at several residues (reviewed in (107)). It was suggested that phosphorylation at S33 is mediated by ATR, while phosphorylation at S4/8 is mediated in a DNA-PK dependent manner (4, 104). Here, we examined spatial localization of the RPA subunit RPA32 and its phosphorylation at S4/8 in infected cells. Our results show that total RPA32 is recruited into HSV-1 and AAV2 RCs (data not shown) and that its expression levels were not altered by virus infection (Fig. 6A). Western analysis of cells, productively infected with either HSV-1 or AAV2 revealed phosphorylation of RPA32 at Ser4/8 only upon AAV2 replication (Fig. 6A). More precisely, RPA32-P-S4/8 clearly co-localized with approximately 70% of small and large AAV2 RCs, but only with 21% of small and 11% of large HSV-1 RCs (Fig. 6, B and C). UV-treated cells served as positive control (Fig. 6B). Moreover, accumulation of RPA32-P-S4/8 was only observed in AAV2 RCs of DNA-PKcs positive cells (Fig. 6D). In summary, these data show that co-infection with AAV2 and HSV-1 induces DNA-PKcs dependent phosphorylation of RPA32 at S4/8.

Discussion

In this study, we compared the phosphorylation status and spatial organization of DDR proteins between cells infected with HSV-1 alone and cells co-infected with HSV-1 and AAV2. Western and immunofluorescence analyses demonstrated that HSV-1 and AAV2 co-infection induced a strong DDR (Table 1 and Fig. 7). Specifically, HSV-1 supported AAV2 replication induced the phosphorylation of Nbs1 and H2AX, as well as ATM and its substrates Chk2 and p53. These responses are similar to those induced by HSV-1 infection alone observed here and in previous studies (13, 49, 67, 76, 81, 95). We also detected phosphorylation of ATR and recruitment of pATR along with its binding partner ATRIP into HSV-1 supported AAV2 RCs as well as into HSV-1 compartments; although kinase activity of ATR was blocked upon HSV-1 and AAV2 replication as we did not detect phosphorylation of Chk1 at the ATR target sites S317 and S345. Our results are similar to a previous study showing that ATR, although recruited together with ATRIP into HSV-1 RCs, is unable to activate Chk1. In addition Mohni et al. showed that, both ATR and ATRIP even if not activated contribute to efficient HSV-1 infection (58).

Due to the strong affinity of RPA32 to single-stranded DNA (102, 107) and its function in recruiting the ATRIP-ATR complex to sites of DNA damage (7, 26, 106), it is not surprising that we and others (65, 79) detected RPA32 in HSV-1 supported AAV2 RCs. In HSV-1 infected cells, RPA32 co-localizes with the HSV-1 major single-stranded DNA binding protein ICP8 (81) in HSV-1 RCs (82, 93). Replicating HSV-1 DNA contains stretches of single stranded DNA (39) which may recruit RPA32 into HSV-1 RCs also independently of ICP8. Single stranded DNA binding proteins such as RPA32 are proposed to stimulate AAV2 DNA replication (64, 79), e.g. by protecting the single-stranded replication products from nucleases (63) and by enhancing binding and nicking of Rep proteins at the replication origins (79).

HSV-1 has been demonstrated to induce the degradation of DNA-PKcs in an ICP0 dependent manner (48, 67). Although Western analysis of total infected cells displayed a similar degradation of DNA-PKcs, in cells infected with HSV-1 or co-infected with HSV-1 and AAV2, a striking difference was observed at the single cell level as well as in cells productively infected with HSV-1 and AAV2 captured by FACS. Flow cytometry, immunofluorescence analysis, and Western analysis of sorted cells revealed an AAV2 mediated delay in the HSV-1 dependent degradation of DNA-PKcs as well as an AAV2 induced phosphorylation of DNA-PKcs. The observed discrepancy in the results obtained with Western blots of total cell lysates and analyses on the single cell level is likely due to the fact that, under the chosen experimental conditions, only approximately 10% of the cells supported AAV2 replication. In order to estimate the extent of the delay in DNA-PKcs degradation, we co-visualized DNA-PKcs and the HSV-1 immediate-early (IE) and early (E) proteins ICP0 and ICP8, respectively, which allow monitoring the progression of HSV-1 infection. While DNA-PKcs and ICP0 or ICP8 were not co-detected in cells infected with HSV-1 alone, DNA-PKcs and ICP0 or ICP8 were consistently co-detected in cells co-infected with HSV-1 and AAV2, and they co-localized with AAV2 RCs. As we did not observe an AAV2-mediated inhibition of ICP0 in this study (Fig. S1B) and in a previous study (31), we speculate that AAV2 replication can prevent the ICP0 dependent degradation of DNA-PKcs (48, 67) e.g. by shielding DNA-PKcs in viral RCs. We can exclude the possibility, that AAV2 replication directly inhibits the E3 ubiquitin ligase activity of ICP0 because USP7, another target of ICP0-mediated proteasomal degradation (12), was rapidly degraded in co-infected cells. In addition, we can exclude a possible role of USP7 in preventing degradation of DNA-PKcs by deubiquitinating (45) DNA-PKcs. Experiments performed with ATM-deficient cells revealed that the AAV2 mediated delay of DNA-PKcs degradation affected downstream signaling via Chk2 and p53. In these cells, co-infection with both viruses resulted in a DDR comparable to that induced by infection with HSV-1ΔICP0, including phosphorylation of p53. Consistent with previous data (51, 76), infection of ATM-deficient cells with HSV-1 alone resulted in a broad reduction of DDR signaling with undetectable levels of Chk2-P-T86 and p53-P-S15. We therefore hypothesize that in co-infected ATM-deficient cells, DNA-PK is responsible for the phosphorylation of Chk2 and p53 (Fig. 7). A role for DNA-PK in the phosphorylation of Chk2 and p53 has previously been reported (49, 50, 85, 86, 88). In fact, here, we demonstrate that DNA-PK is essential for the activation of p53 in cells infected with AAV2 alone (Figs. 1C and 5A).

Recently, we reported hyperphosphorylation of RPA32 at the DNA-PK target-site S4/8 in cells transfected with plasmids encoding the AAV2 Rep68 or Rep78 proteins (30). In the present study, we detected phosphorylation of RPA32 at S4/8 and recruitment of RPA32-P-S4/8 into HSV-1 supported AAV2 RCs. In contrast, HSV-1 infection alone did not induce phosphorylation of RPA32 at S4/8. Similar to the phosphorylation of Chk2 and p53 in co-infected cells, phosphorylation of RPA32 at S4/8 may also be a consequence of the delayed degradation of DNA-PKcs. Further support for this theory comes from the fact that DNA-PK has previously been demonstrated to phosphorylate RPA32 at S4/8 (4, 11, 104).

By comparing our results in co-infected cells with previous studies examining the DDR signaling in cells infected with HSV-1 alone (13, 51, 76, 96), Ad2 alone (17, 78) or co-infected with AAV2 and Ad2 (25, 75), it is remarkable that although Ad and HSV-1 by themselves induce very different DDR, in the presence of AAV2, the induction and activation pattern of DDR proteins are more similar. It seems that during AAV2 replication, the cellular DDR is modulated towards a DNA-PK-dependent signaling, which might have positive and/or negative impact on AAV replication and transduction, depending on the cellular environment and the viral genome structure (23, 25, 75). Further experiments will address the question whether this modulation can enhance HSV-1 supported AAV2 replication and/or inhibit helper virus replication.

Acknowledgments

We thank P. Beard (ETH, Lausanne, Switzerland) for helpful discussions and A. Nicolas (INSERM, Lyon, France) for critically reading the manuscript. We are also grateful to E. Hendrickson, T. Melendy, Y. Shiloh, and P. Nghiem for providing cell lines and B. Roizman, N. Stow, R.D. Everett, H. Buening, U. Greber, and M. Linden for providing viruses. This work was supported by the Swiss National Science Foundation grant No.31003A_124938 to C.F. D.L.G. is supported by fellowships from the Swiss National Science Foundation and the Swiss Foundation for Grants in Biology and Medicine (PBZHP3-122925 and PASMP3-132554). A.S. and N.J. are supported by INSERM and the Association Française contre les Myopathies (AFM). Work in the Weitzman laboratory was partially supported by a Pioneer Developmental Chair from the Salk Institute and by NIH grants CA97093 and AI43341 (M.D.W.).

References

1. **Adeyemi, R. O., S. Landry, M. E. Davis, M. D. Weitzman, and D. J. Pintel.** 2010 Parvovirus minute virus of mice induces a DNA damage response that facilitates viral replication. PLoS Pathog **6:**e1001141.
2. **Ahn, J. Y., J. K. Schwarz, H. Piwnica-Worms, and C. E. Canman.** 2000. Threonine 68 phosphorylation by ataxia telangiectasia mutated is required for efficient activation of Chk2 in response to ionizing radiation. Cancer Res **60:**5934-6.
3. **Alazard-Dany, N., A. Nicolas, A. Ploquin, R. Strasser, A. Greco, A. L. Epstein, C. Fraefel, and A. Salvetti.** 2009. Definition of herpes simplex virus type 1 helper activities for adeno-associated virus early replication events. PLoS Pathog **5:**e1000340.
4. **Anantha, R. W., V. M. Vassin, and J. A. Borowiec.** 2007. Sequential and synergistic modification of human RPA stimulates chromosomal DNA repair. J Biol Chem **282:**35910-23.
5. **Antoni, B. A., A. B. Rabson, I. L. Miller, J. P. Trempe, N. Chejanovsky, and B. J. Carter.** 1991. Adeno-associated virus Rep protein inhibits human immunodeficiency virus type 1 production in human cells. J Virol **65:**396-404.
6. **Bakkenist, C. J., and M. B. Kastan.** 2003. DNA damage activates ATM through intermolecular autophosphorylation and dimer dissociation. Nature **421:**499-506.
7. **Ball, H. L., J. S. Myers, and D. Cortez.** 2005. ATRIP binding to replication protein A-single-stranded DNA promotes ATR-ATRIP localization but is dispensable for Chk1 phosphorylation. Mol Biol Cell **16:**2372-81.
8. **Banin, S., L. Moyal, S. Shieh, Y. Taya, C. W. Anderson, L. Chessa, N. I. Smorodinsky, C. Prives, Y. Reiss, Y. Shiloh, and Y. Ziv.** 1998. Enhanced phosphorylation of p53 by ATM in response to DNA damage. Science **281:**1674-7.
9. **Berthet, C., K. Raj, P. Saudan, and P. Beard.** 2005. How adeno-associated virus Rep78 protein arrests cells completely in S phase. Proc Natl Acad Sci U S A **102:**13634-9.
10. **Binz, S. K., A. M. Sheehan, and M. S. Wold.** 2004. Replication protein A phosphorylation and the cellular response to DNA damage. DNA Repair (Amst) **3:**1015-24.
11. **Block, W. D., Y. Yu, and S. P. Lees-Miller.** 2004. Phosphatidyl inositol 3-kinase-like serine/threonine protein kinases (PIKKs) are required for DNA damage-induced phosphorylation of the 32 kDa subunit of replication protein A at threonine 21. Nucleic Acids Res **32:**997-1005.
12. **Boutell, C., M. Canning, A. Orr, and R. D. Everett.** 2005. Reciprocal activities between herpes simplex virus type 1 regulatory protein ICP0, a ubiquitin E3 ligase, and ubiquitin-specific protease USP7. J Virol **79:**12342-54.
13. **Boutell, C., and R. D. Everett.** 2004. Herpes simplex virus type 1 infection induces the stabilization of p53 in a USP7- and ATM-independent manner. J Virol **78:**8068-77.
14. **Buller, R. M., J. E. Janik, E. D. Sebring, and J. A. Rose.** 1981. Herpes simplex virus types 1 and 2 completely help adenovirus-associated virus

replication. J Virol **40:**241-7.

15. **Burma, S., B. P. Chen, and D. J. Chen.** 2006. Role of non-homologous end joining (NHEJ) in maintaining genomic integrity. DNA Repair (Amst) **5:**1042-8.
16. **Cahill, D., B. Connor, and J. P. Carney.** 2006. Mechanisms of eukaryotic DNA double strand break repair. Front Biosci **11:**1958-76.
17. **Carson, C. T., R. A. Schwartz, T. H. Stracker, C. E. Lilley, D. V. Lee, and M. D. Weitzman.** 2003. The Mre11 complex is required for ATM activation and the G2/M checkpoint. Embo J **22:**6610-20.
18. **Cataldi, M. P., and D. M. McCarty.** 2010. Differential effects of DNA double-strand break repair pathways on single-strand and self-complementary adeno-associated virus vector genomes. J Virol **84:**8673-82.
19. **Chan, D. W., B. P. Chen, S. Prithivirajsingh, A. Kurimasa, M. D. Story, J. Qin, and D. J. Chen.** 2002. Autophosphorylation of the DNA-dependent protein kinase catalytic subunit is required for rejoining of DNA double-strand breaks. Genes Dev **16:**2333-8.
20. **Chaturvedi, P., W. K. Eng, Y. Zhu, M. R. Mattern, R. Mishra, M. R. Hurle, X. Zhang, R. S. Annan, Q. Lu, L. F. Faucette, G. F. Scott, X. Li, S. A. Carr, R. K. Johnson, J. D. Winkler, and B. B. Zhou.** 1999. Mammalian Chk2 is a downstream effector of the ATM-dependent DNA damage checkpoint pathway. Oncogene **18:**4047-54.
21. **Chen, B. P., D. W. Chan, J. Kobayashi, S. Burma, A. Asaithamby, K. Morotomi-Yano, E. Botvinick, J. Qin, and D. J. Chen.** 2005. Cell cycle dependence of DNA-dependent protein kinase phosphorylation in response to DNA double strand breaks. J Biol Chem **280:**14709-15.
22. **Chen, Y., and Y. Sanchez.** 2004. Chk1 in the DNA damage response: conserved roles from yeasts to mammals. DNA Repair (Amst) **3:**1025-32.
23. **Choi, Y. K., K. Nash, B. J. Byrne, N. Muzyczka, and S. Song.** 2010. The effect of DNA-dependent protein kinase on adeno-associated virus replication. PLoS One **5:**e15073.
24. **Clarke, P. R., and L. A. Allan.** 2009. Cell-cycle control in the face of damage--a matter of life or death. Trends Cell Biol **19:**89-98.
25. **Collaco, R. F., J. M. Bevington, V. Bhrigu, V. Kalman-Maltese, and J. P. Trempe.** 2009. Adeno-associated virus and adenovirus coinfection induces a cellular DNA damage and repair response via redundant phosphatidylinositol 3-like kinase pathways. Virology **392:**24-33.
26. **Dart, D. A., K. E. Adams, I. Akerman, and N. D. Lakin.** 2004. Recruitment of the cell cycle checkpoint kinase ATR to chromatin during S-phase. J Biol Chem **279:**16433-40.
27. **Daya, S., N. Cortez, and K. I. Berns.** 2009. Adeno-associated virus site-specific integration is mediated by proteins of the nonhomologous end-joining pathway. J Virol **83:**11655-64.
28. **Fraefel, C., A. G. Bittermann, H. Bueler, I. Heid, T. Bachi, and M. Ackermann.** 2004. Spatial and temporal organization of adeno-associated virus DNA replication in live cells. J Virol **78:**389-98.
29. **Giglia-Mari, G., A. Zotter, and W. Vermeulen.** 2010. DNA damage response. Cold Spring Harb Perspect Biol **3:**a000745.
30. **Glauser, D. L., M. Seyffert, R. Strasser, M. Franchini, A. S. Laimbacher, C. Dresch, A. P. de Oliveira, R. Vogel, H. Buning, A. Salvetti, M. Ackermann, and C. Fraefel.** 2010. Inhibition of herpes simplex virus type 1 replication by

adeno-associated virus rep proteins depends on their combined DNA-binding and ATPase/helicase activities. J Virol **84:**3808-24.

31. **Glauser, D. L., R. Strasser, A. S. Laimbacher, O. Saydam, N. Clement, R. M. Linden, M. Ackermann, and C. Fraefel.** 2007. Live covisualization of competing adeno-associated virus and herpes simplex virus type 1 DNA replication: molecular mechanisms of interaction. J Virol **81:**4732-43.
32. **Guo, Z., A. Kumagai, S. X. Wang, and W. G. Dunphy.** 2000. Requirement for Atr in phosphorylation of Chk1 and cell cycle regulation in response to DNA replication blocks and UV-damaged DNA in Xenopus egg extracts. Genes Dev **14:**2745-56.
33. **Harper, J. W., and S. J. Elledge.** 2007. The DNA damage response: ten years after. Mol Cell **28:**739-45.
34. **Heilbronn, R., A. Burkle, S. Stephan, and H. zur Hausen.** 1990. The adeno-associated virus rep gene suppresses herpes simplex virus-induced DNA amplification. J Virol **64:**3012-8.
35. **Heilbronn, R., M. Engstler, S. Weger, A. Krahn, C. Schetter, and M. Boshart.** 2003. ssDNA-dependent colocalization of adeno-associated virus Rep and herpes simplex virus ICP8 in nuclear replication domains. Nucleic Acids Res **31:**6206-13.
36. **Helleday, T., J. Lo, D. C. van Gent, and B. P. Engelward.** 2007. DNA double-strand break repair: from mechanistic understanding to cancer treatment. DNA Repair (Amst) **6:**923-35.
37. **Hunter, L. A., and R. J. Samulski.** 1992. Colocalization of adeno-associated virus Rep and capsid proteins in the nuclei of infected cells. J Virol **66:**317-24.
38. **Jackson, S. P., and J. Bartek.** 2009. The DNA-damage response in human biology and disease. Nature **461:**1071-8.
39. **Jacob, R. J., and B. Roizman.** 1977. Anatomy of herpes simplex virus DNA VIII. Properties of the replicating DNA. J Virol **23:**394-411.
40. **Jing, X. J., V. Kalman-Maltese, X. Cao, Q. Yang, and J. P. Trempe.** 2001. Inhibition of adenovirus cytotoxicity, replication, and E2a gene expression by adeno-associated virus. Virology **291:**140-51.
41. **Jurvansuu, J., K. Raj, A. Stasiak, and P. Beard.** 2005. Viral transport of DNA damage that mimics a stalled replication fork. J Virol **79:**569-80.
42. **Kastan, M. B., and D. S. Lim.** 2000. The many substrates and functions of ATM. Nat Rev Mol Cell Biol **1:**179-86.
43. **Kastan, M. B., D. S. Lim, S. T. Kim, B. Xu, and C. Canman.** 2000. Multiple signaling pathways involving ATM. Cold Spring Harb Symp Quant Biol **65:**521-6.
44. **Kleinschmidt, J. A., M. Mohler, F. W. Weindler, and R. Heilbronn.** 1995. Sequence elements of the adeno-associated virus rep gene required for suppression of herpes-simplex-virus-induced DNA amplification. Virology **206:**254-62.
45. **Komander, D., M. J. Clague, and S. Urbe.** 2009. Breaking the chains: structure and function of the deubiquitinases. Nat Rev Mol Cell Biol **10:**550-63.
46. **Lakin, N. D., B. C. Hann, and S. P. Jackson.** 1999. The ataxia-telangiectasia related protein ATR mediates DNA-dependent phosphorylation of p53. Oncogene **18:**3989-95.
47. **Lamarche, B. J., N. I. Orazio, and M. D. Weitzman.** 2010. The MRN complex in double-strand break repair and telomere maintenance. FEBS Lett

584:3682-95.

48. **Lees-Miller, S. P., M. C. Long, M. A. Kilvert, V. Lam, S. A. Rice, and C. A. Spencer.** 1996. Attenuation of DNA-dependent protein kinase activity and its catalytic subunit by the herpes simplex virus type 1 transactivator ICP0. J Virol **70:**7471-7.

49. **Lees-Miller, S. P., K. Sakaguchi, S. J. Ullrich, E. Appella, and C. W. Anderson.** 1992. Human DNA-activated protein kinase phosphorylates serines 15 and 37 in the amino-terminal transactivation domain of human p53. Mol Cell Biol **12:**5041-9.

50. **Li, J., and D. F. Stern.** 2005. Regulation of CHK2 by DNA-dependent protein kinase. J Biol Chem **280:**12041-50.

51. **Lilley, C. E., C. T. Carson, A. R. Muotri, F. H. Gage, and M. D. Weitzman.** 2005. DNA repair proteins affect the lifecycle of herpes simplex virus 1. Proc Natl Acad Sci U S A **102:**5844-9.

52. **Linden, R. M., and K. I. Berns.** 2000. Molecular biology of adeno-associated viruses. Contrib Microbiol **4:**68-84.

53. **Liu, Q., S. Guntuku, X. S. Cui, S. Matsuoka, D. Cortez, K. Tamai, G. Luo, S. Carattini-Rivera, F. DeMayo, A. Bradley, L. A. Donehower, and S. J. Elledge.** 2000. Chk1 is an essential kinase that is regulated by Atr and required for the G(2)/M DNA damage checkpoint. Genes Dev **14:**1448-59.

54. **Liu, S., B. Shiotani, M. Lahiri, A. Marechal, A. Tse, C. C. Leung, J. N. Glover, X. H. Yang, and L. Zou.** ATR autophosphorylation as a molecular switch for checkpoint activation. Mol Cell **43:**192-202.

55. **Lovejoy, C. A., and D. Cortez.** 2009. Common mechanisms of PIKK regulation. DNA Repair (Amst) **8:**1004-8.

56. **Matsuoka, S., M. Huang, and S. J. Elledge.** 1998. Linkage of ATM to cell cycle regulation by the Chk2 protein kinase. Science **282:**1893-7.

57. **Matsuoka, S., G. Rotman, A. Ogawa, Y. Shiloh, K. Tamai, and S. J. Elledge.** 2000. Ataxia telangiectasia-mutated phosphorylates Chk2 in vivo and in vitro. Proc Natl Acad Sci U S A **97:**10389-94.

58. **Mohni, K. N., C. M. Livingston, D. Cortez, and S. K. Weller.** 2010. ATR and ATRIP are recruited to herpes simplex virus type 1 replication compartments even though ATR signaling is disabled. J Virol **84:**12152-64.

59. **Mordes, D. A., and D. Cortez.** 2008. Activation of ATR and related PIKKs. Cell Cycle **7:**2809-12.

60. **Morio, T., and H. Kim.** 2008. Ku, Artemis, and ataxia-telangiectasia-mutated: signalling networks in DNA damage. Int J Biochem Cell Biol **40:**598-603.

61. **Nada, S., and J. P. Trempe.** 2002. Characterization of adeno-associated virus rep protein inhibition of adenovirus E2a gene expression. Virology **293:**345-55.

62. **Nam, E. A., and D. Cortez.** ATR signalling: more than meeting at the fork. Biochem J **436:**527-36.

63. **Nash, K., W. Chen, M. Salganik, and N. Muzyczka.** 2009. Identification of cellular proteins that interact with the adeno-associated virus rep protein. J Virol **83:**454-69.

64. **Ni, T. H., W. F. McDonald, I. Zolotukhin, T. Melendy, S. Waga, B. Stillman, and N. Muzyczka.** 1998. Cellular proteins required for adeno-associated virus DNA replication in the absence of adenovirus coinfection. J Virol **72:**2777-87.

65. **Nicolas, A., N. Alazard-Dany, C. Biollay, L. Arata, N. Jolinon, L. Kuhn, M.**

Ferro, S. K. Weller, A. L. Epstein, A. Salvetti, and A. Greco. 2010. Identification of Rep-Associated Factors in Hsv-1-Induced Aav-2 Replication Compartments. J Virol.

66. **Ohnishi, T., E. Mori, and A. Takahashi.** 2009. DNA double-strand breaks: their production, recognition, and repair in eukaryotes. Mutat Res **669:**8-12.
67. **Parkinson, J., S. P. Lees-Miller, and R. D. Everett.** 1999. Herpes simplex virus type 1 immediate-early protein vmw110 induces the proteasome-dependent degradation of the catalytic subunit of DNA-dependent protein kinase. J Virol **73:**650-7.
68. **Raj, K., P. Ogston, and P. Beard.** 2001. Virus-mediated killing of cells that lack p53 activity. Nature **412:**914-7.
69. **Reinhardt, H. C., and M. B. Yaffe.** 2009. Kinases that control the cell cycle in response to DNA damage: Chk1, Chk2, and MK2. Curr Opin Cell Biol **21:**245-55.
70. **Robinson, K., N. Asawachaicharn, D. A. Galloway, and C. Grandori.** 2009. c-Myc accelerates S-Phase and requires WRN to avoid replication stress. PLoS One **4:**e5951.
71. **Rommelaere, J., and J. J. Cornelis.** 1991. Antineoplastic activity of parvoviruses. J Virol Methods **33:**233-51.
72. **Samulski, R. J., X. Zhu, X. Xiao, J. D. Brook, D. E. Housman, N. Epstein, and L. A. Hunter.** 1991. Targeted integration of adeno-associated virus (AAV) into human chromosome 19. Embo J **10:**3941-50.
73. **Saudan, P., J. Vlach, and P. Beard.** 2000. Inhibition of S-phase progression by adeno-associated virus Rep78 protein is mediated by hypophosphorylated pRb. Embo J **19:**4351-61.
74. **Schlehofer, J. R.** 1994. The tumor suppressive properties of adeno-associated viruses. Mutat Res **305:**303-13.
75. **Schwartz, R. A., C. T. Carson, C. Schuberth, and M. D. Weitzman.** 2009. Adeno-associated virus replication induces a DNA damage response coordinated by DNA-dependent protein kinase. J Virol **83:**6269-78.
76. **Shirata, N., A. Kudoh, T. Daikoku, Y. Tatsumi, M. Fujita, T. Kiyono, Y. Sugaya, H. Isomura, K. Ishizaki, and T. Tsurumi.** 2005. Activation of ataxia telangiectasia-mutated DNA damage checkpoint signal transduction elicited by herpes simplex virus infection. J Biol Chem **280:**30336-41.
77. **Song, S., Y. Lu, Y. K. Choi, Y. Han, Q. Tang, G. Zhao, K. I. Berns, and T. R. Flotte.** 2004. DNA-dependent PK inhibits adeno-associated virus DNA integration. Proc Natl Acad Sci U S A **101:**2112-6.
78. **Stracker, T. H., C. T. Carson, and M. D. Weitzman.** 2002. Adenovirus oncoproteins inactivate the Mre11-Rad50-NBS1 DNA repair complex. Nature **418:**348-52.
79. **Stracker, T. H., G. D. Cassell, P. Ward, Y. M. Loo, B. van Breukelen, S. D. Carrington-Lawrence, R. K. Hamatake, P. C. van der Vliet, S. K. Weller, T. Melendy, and M. D. Weitzman.** 2004. The Rep protein of adeno-associated virus type 2 interacts with single-stranded DNA-binding proteins that enhance viral replication. J Virol **78:**441-53.
80. **Tapia-Alveal, C., T. M. Calonge, and M. J. O'Connell.** 2009. Regulation of chk1. Cell Div **4:**8.
81. **Taylor, T. J., and D. M. Knipe.** 2004. Proteomics of herpes simplex virus replication compartments: association of cellular DNA replication, repair,

recombination, and chromatin remodeling proteins with ICP8. J Virol **78:**5856-66.

82. **Taylor, T. J., E. E. McNamee, C. Day, and D. M. Knipe.** 2003. Herpes simplex virus replication compartments can form by coalescence of smaller compartments. Virology **309:**232-47.
83. **Tibbetts, R. S., D. Cortez, K. M. Brumbaugh, R. Scully, D. Livingston, S. J. Elledge, and R. T. Abraham.** 2000. Functional interactions between BRCA1 and the checkpoint kinase ATR during genotoxic stress. Genes Dev **14:**2989-3002.
84. **Timpe, J. M., K. C. Verrill, and J. P. Trempe.** 2006. Effects of adeno-associated virus on adenovirus replication and gene expression during coinfection. J Virol **80:**7807-15.
85. **Tomimatsu, N., B. Mukherjee, and S. Burma.** 2009. Distinct roles of ATR and DNA-PKcs in triggering DNA damage responses in ATM-deficient cells. EMBO Rep **10:**629-35.
86. **Wang, S., M. Guo, H. Ouyang, X. Li, C. Cordon-Cardo, A. Kurimasa, D. J. Chen, Z. Fuks, C. C. Ling, and G. C. Li.** 2000. The catalytic subunit of DNA-dependent protein kinase selectively regulates p53-dependent apoptosis but not cell-cycle arrest. Proc Natl Acad Sci U S A **97:**1584-8.
87. **Wang, X. Q., J. L. Redpath, S. T. Fan, and E. J. Stanbridge.** 2006. ATR dependent activation of Chk2. J Cell Physiol **208:**613-9.
88. **Wang, Y., and W. Eckhart.** 1992. Phosphorylation sites in the amino-terminal region of mouse p53. Proc Natl Acad Sci U S A **89:**4231-5.
89. **Warmerdam, D. O., and R. Kanaar.** 2010. Dealing with DNA damage: relationships between checkpoint and repair pathways. Mutat Res **704:**2-11.
90. **Weindler, F. W., and R. Heilbronn.** 1991. A subset of herpes simplex virus replication genes provides helper functions for productive adeno-associated virus replication. J Virol **65:**2476-83.
91. **Weitzman, M. D., K. J. Fisher, and J. M. Wilson.** 1996. Recruitment of wild-type and recombinant adeno-associated virus into adenovirus replication centers. J Virol **70:**1845-54.
92. **Weitzman, M. D., C. E. Lilley, and M. S. Chaurushiya.** 2009. Genomes in conflict: maintaining genome integrity during virus infection. Annu Rev Microbiol **64:**61-81.
93. **Wilcock, D., and D. P. Lane.** 1991. Localization of p53, retinoblastoma and host replication proteins at sites of viral replication in herpes-infected cells. Nature **349:**429-31.
94. **Wilkinson, D. E., and S. K. Weller.** 2006. Herpes simplex virus type I disrupts the ATR-dependent DNA-damage response during lytic infection. J Cell Sci **119:**2695-703.
95. **Wilkinson, D. E., and S. K. Weller.** 2005. Inhibition of the herpes simplex virus type 1 DNA polymerase induces hyperphosphorylation of replication protein A and its accumulation at S-phase-specific sites of DNA damage during infection. J Virol **79:**7162-71.
96. **Wilkinson, D. E., and S. K. Weller.** 2004. Recruitment of cellular recombination and repair proteins to sites of herpes simplex virus type 1 DNA replication is dependent on the composition of viral proteins within prereplicative sites and correlates with the induction of the DNA damage response. J Virol **78:**4783-96.

97. **Wold, M. S.** 1997. Replication protein A: a heterotrimeric, single-stranded DNA-binding protein required for eukaryotic DNA metabolism. Annu Rev Biochem **66:**61-92.
98. **Wold, M. S., and T. Kelly.** 1988. Purification and characterization of replication protein A, a cellular protein required for in vitro replication of simian virus 40 DNA. Proc Natl Acad Sci U S A **85:**2523-7.
99. **Wyman, C., and R. Kanaar.** 2006. DNA double-strand break repair: all's well that ends well. Annu Rev Genet **40:**363-83.
100. **Yang, Q., F. Chen, J. Ross, and J. P. Trempe.** 1995. Inhibition of cellular and SV40 DNA replication by the adeno-associated virus Rep proteins. Virology **207:**246-50.
101. **Yang, Q., F. Chen, and J. P. Trempe.** 1994. Characterization of cell lines that inducibly express the adeno-associated virus Rep proteins. J Virol **68:**4847-56.
102. **You, J. S., M. Wang, and S. H. Lee.** 2000. Functional characterization of zinc-finger motif in redox regulation of RPA-ssDNA interaction. Biochemistry **39:**12953-8.
103. **You, Z., C. Chahwan, J. Bailis, T. Hunter, and P. Russell.** 2005. ATM activation and its recruitment to damaged DNA require binding to the C terminus of Nbs1. Mol Cell Biol **25:**5363-79.
104. **Zernik-Kobak, M., K. Vasunia, M. Connelly, C. W. Anderson, and K. Dixon.** 1997. Sites of UV-induced phosphorylation of the p34 subunit of replication protein A from HeLa cells. J Biol Chem **272:**23896-904.
105. **Zhao, H., and H. Piwnica-Worms.** 2001. ATR-mediated checkpoint pathways regulate phosphorylation and activation of human Chk1. Mol Cell Biol **21:**4129-39.
106. **Zou, L., and S. J. Elledge.** 2003. Sensing DNA damage through ATRIP recognition of RPA-ssDNA complexes. Science **300:**1542-8.
107. **Zou, Y., Y. Liu, X. Wu, and S. M. Shell.** 2006. Functions of human replication protein A (RPA): from DNA replication to DNA damage and stress responses. J Cell Physiol **208:**267-73.

Figure legends

Figure 1. DNA damage signaling induced by viral infection. (A-C) Western analysis of infected cell lysates. MO59J Fus1 cells were either mock-infected (m) or infected with AAV2 alone (MOI 2000), HSV-1 alone (MOI 1.5), or co-infected with AAV2 (MOI 2000) and HSV-1 (MOI 1.5) and harvested at the indicated hours post infection (hpi). Total proteins were extracted, separated by SDS-PAGE, blotted onto nitrocellulose membrane, and analyzed with the indicated antibodies. Actin served as a loading control; detection of HSV-1 ICP8 and AAV2 Rep was used as an infection control.

Figure 2. Activation of primary DNA damage response proteins. MO59J Fus1 cells were either mock-infected or infected with HSV-1 (MOI 1.5), or co-infected with rAAVCR (MOI 250) and HSV-1 (MOI 1.5). After 24 h, cells were fixed and processed for immunofluorescence analysis. rAAVCR replication compartments (AAV RCs) were visualized by binding of the rAAVCR encoded mCherry-Rep68/78 fusion protein (CR) to AAV DNA (red). HSV-1 RCs were visualized with a primary antibody specific for the HSV-1 major DNA binding protein ICP8 and an AF594-labeled secondary antibody (red). Cells treated with HU (3mM) served as DDR control. To identify phosphorylated Nbs1 **(A)** and H2AX **(B)**, cells were stained with antibodies specific for Nbs1-P-S343 or H2AX-P-S139 (γH2AX) and a FITC-labeled secondary antibody (green). DAPI was used to stain cellular DNA. Images were taken using a confocal laser scanning microscope and represent a single optical z slice of the nuclei. Scale bar = 10 µm.

Figure 3. Recruitment of ATM-P-S1981, ATR-P-S428, and ATRIP into HSV-1 and AAV2 RCs. MO59J Fus1 cells were infected and processed for immunofluorescence, and viral RCs (red) were visualized as described in Fig. 2. Cells were stained with an antibody specific for (**A**) ATM-P-S1981, (**B**) ATR-P-S428, or (**C**) ATRIP and a FITC-labeled secondary antibody (green). DAPI was used to

stain cell nuclei. In A, cells deficient for ATM (AT-22 IJE T) served as a control for the phosphospecific ATM-antibody. In B, the percentage of ATR-P-S428 in viral RCs is indicated. Scale bar = 10 µm.

Figure 4. Activation and delayed degradation of DNA-PKcs in cells co-infected with HSV-1 and AAV2. **(A)** MO59J Fus1 cells were infected with HSV-1 (MOI 1.5), HSV-1ΔICP0 (MOI 0.9), or mock-infected. After 24 h, cells were fixed and processed for immunofluorescence analysis. HSV-1 infection was detected using an antibody specific for ICP0 or ICP8 and an AF594-labeled secondary antibody (red). Additionally, cells were stained with an antibody specific for DNA-PKcs and a FITC-labeled secondary antibody (green). DAPI was used to stain cellular DNA. Scale bar = 10 µm. **(B)** Immunofluorescence analysis of MO59J Fus1 cells at 24 h after co-infection with rAAVCR (MOI 250) and HSV-1 (MOI 1.5). rAAVCR RCs (red) were visualized as described in Fig. 2. Additionally, cells were stained with antibodies specific for ICP0 or ICP8 and an AF405-labeled secondary antibody (purple) and with an antibody specific for DNA-PKcs and an FITC-labeled secondary antibody (green). The percentage of DNA-PKcs in rAAVCR RCs is indicated. Scale bar = 10 µm. **(C)** Flow cytometric analysis of infected cells. DNA-PKcs positive HCT116 cells were mock infected (positive control), infected with rHSV-1ICP4eYFP (MOI 1.5) or co-infected with HSV-1 (MOI 1.5), AAV2 (MOI 250), and rAAVGFP (MOI 250). HCT116 cells negative for DNA-PKcs, served as negative control. Cells were fixed 20 h post-infection and stained with a monoclonal DNA-PKcs-specific antibody and a Cy5-labeled secondary antibody. DNA-PKcs was analyzed in HSV-1-infected cells positive for EYFP-ICP4 (HSV) and in co-infected cells positive for EGFP (HSV+AAV). A minimum of 80`0000 events were scored for each sample. Graphs were overlayed to show the fluorescence shift of HSV-1 infected populations. **(D and E)** Western analysis of AT22IJE-T cells, sorted for productive HSV-1 and AAV2 infection at 22 and 26 hpi. Cells were mock-infected, infected with rHSV-1vECFP-ICP4 (rHSV; MOI 2), or co-infected (rHSV + rAAV) with rHSV-1vECFP-ICP4 (MOI 2) and rAAV2CR (MOI 4000). Lysates of sorted cells were processed for Western analysis and stained with the indicated antibodies. Quantification of Western blot band intensities was done with a gel doc system using Quantity One® software (Version 4.6.1;

BioRad; Hercules; CA; USA). **(F)** Western analysis of AT22IJE-T cells, sorted for productive HSV-1 and AAV2 infection at 24hpi. Cells were mock-infected, infected with rHSV-1vECFP-ICP4 (rHSV; MOI 4), or co-infected (rHSV + rAAV) with rHSV-1vECFP-ICP4 (MOI 4) and rAAV2CR (MOI 4000). Lysates of sorted cells were processed for Western analysis and stained with the indicated antibodies. **(G)** MO59J Fus1 cells were mock-infected, infected with HSV-1 (MOI 1.5), or co-infected with rAAVCR (MOI 250) and either HSV-1 (MOI 1.5) or Ad2 (MOI 12.5). After 24 h, cells were fixed and processed for immunofluorescence analysis. rAAVCR and HSV-1 RCs (red) were visualized as described in Fig. 2. DNA-PKcs-phosphorylation was detected with an antibody specific for DNA-PKcs-P-S2056 and a FITC-labeled secondary antibody (green). As negative control, MO59J Fus9 DNA-PKcs-negative cells were co-infected with rAAVCR (MOI 250) and Ad2 (MOI 12.5) and stained for pDNA-PKcs. DAPI was used to stain cellular DNA. Scale bar = 10 µm.

Figure 5. DNA-PKcs and ATM dependent activation of Chk2 and p53 upon viral infection. (A) Western analysis of DNA-PKcs-deficient MO59J Fus9 cells. Cells were mock-infected or infected with AAV2 (MOI 2000), HSV-1 (MOI 1.5), or co-infected with AAV2 (MOI 2000) and HSV-1 (MOI 1.5). Total proteins were extracted at the indicated hpi and subjected to Western analysis using antibodies specific for actin (loading control), ICP8 (HSV-1 infection control), Chk2, Chk2-P-T68, and p53-P-S15. **(B)** Immunoprecipitation and Western analysis of ATM-negative AT22 IJE-T cells at 24 h after mock-infection (m) or infection with AAV2 (MOI 2000), HSV-1 (MOI 1.5), AAV2 (MOI 2000) and HSV-1 (MOI 1.5). Lysates were analyzed using the indicated antibodies. **(C)** Immunofluorescence analysis of ATM-negative AT22 IJE-T cells at 24 h after infection with HSV-1 (MOI 1.5), rAAVCR (MOI 250) and HSV-1 (MOI 1.5), HSV-1ΔICP0 (MOI 0.9), or mock-infection. rAAVCR and HSV-1 RCs (red) were visualized as described in Fig. 2. p53-activation was detected with an antibody specific for p53-P-S15 and an FITC-labeled secondary antibody (green). DAPI was used to stain cellular nuclei. Scale bar = 10 µm.

Figure 6. Phosphorylation of RPA32 upon AAV2 and HSV-1 replication. (A)

Western analysis of sorted AT22IJE-T cells at 24 hpi. Cells were mock-infected, infected with rHSV-1vECFP-ICP4 (rHSV; MOI 4), or co-infected (rHSV + rAAV) with rHSV-1vECFP-ICP4 (MOI 4) and rAAV2CR (MOI 4000). Sorted cells were subjected to Western analysis and analyzed with the indicated antibodies. **(B)** Immunofluorescence analysis of U2OS cells after infection with HSV-1 (MOI 1.5), rAAVCR (MOI 250) and HSV-1 (MOI 1.5), or mock-infection at 24 h. UV-treated cells (10J/m^2) served as positive control. rAAVCR and HSV-1 RCs (red) were visualized as described in Fig. 2. To detect phosphorylated RPA32, cells were stained with an antibody specific for RPA32-P-S4/8 and a FITC-labeled secondary antibody (green). Cellular DNA was stained with DAPI. Scale bar = 10 µm. **(C)** Quantification of RPA32-P-S4/8 co-localization with small and large AAV2 or HSV-1 RCs in U2OS cells. 50 cells per sample were counted. Black columns, RPA32-P-S4/8 positive viral RCs; open columns, RPA32-P-S4/8 negative viral RCs **(D)** Immunofluorescence analysis of MO59J Fus1 or Fus9 (DNA-PKcs-negative) cells at 24 h after mock-infection or co-infection with HSV-1 (MOI 1.5) and rAAVCR (MOI 250). rAAVCR RCs (red) were visualized as described in Fig. 2. Cells were stained with an antibody specific for RPA32-P-S4/8 and an Alexa Fluor405-labeled secondary antibody (blue). Scale bar = 10 µm.

Figure 7. Models for the DDR signaling induced by HSV-1 replication and HSV-1 supported AAV replication. The analysis of the DDR in ATM-deficient-, DNA-PKcs-deficient- and normal cells support the following models: Infection of cells with HSV-1 induces phopshorylation of ATM and ATR, and signaling to their targets Nbs1, H2AX, Chk2, p53, but not to the ATR-target Chk1. In cells infected with HSV-1 alone, DNA-PKcs is rapidly degraded in an HSV-1 ICP0 dependent manner, and no DNA-PKcs-mediated signaling occurs. By contrast, co-infection with HSV-1 and AAV2 induces the activation of DNA-PKcs which enables phosphorylation of RPA32 at S4/8. Further support for the activation of DNA-PKcs in co-infected cells comes from experiments performed in ATM-deficient cells, as in absence of ATM, HSV-1 and AAV2 co-infection still induced the phosphorylation of p53, Chk2, and RPA32 at S4/8. In ATM-deficient cells infected with HSV-1 alone, the DDR signaling is broadly reduced with undetectable levels of Chk2-P-T86 and p53-P-S15 (Lilley et al., 2005;

Shirata et al., 2007).

Vogel et al., Table 1

TABLE 1. **DNA damage signaling in cells infected with HSV-1 or co-infected with HSV-1 and (r)AAV2.**
Summary of data from Western analysis, immunofluorescence analysis, and flow cytometry.

	HSV-1 and (r)AAV2 co-infection				HSV-1 infection			
Protein	**Inhibition**	**Induction**	**Phosph.**	**Local.**	**Inhibition**	**Induction**	**Phosph.**	**Local.**
ATM	-	-	+	NUC+RCs	-	-	+	RCs
ATR	-	-	+	RCs	-	-	+	RCs
ATRIP	-	+	nd	RCs	-	+	nd	RCs
DNA-PKcs	**+**[a]	**-**	**+**	**RCs**	**+**	**-**	**-**	**-**
USP7	+	-	nd	RCs	+	-	nd	nd
H2AX	nd	nd	+	NUC	nd	nd	+	NUC
NBS1	-	-	+	RCs	-	-	+	RCs
RPA32 (P-Ser4/8)	**-**	**-**	**+**	**RCs**	**-**	**-**	**-**	**RCs**
p53	-	+	+	RCs	-	+	+	RCs
Chk1	-	-	-	RCs	-	-	-	RCs
Chk2	-	-	+	RCs	-	-	+	RCs

[a] Inhibition delayed; NUC, nucleus; nd, not done; bold, AAV-induced modulation of DDR.

Vogel et al., Fig. 1

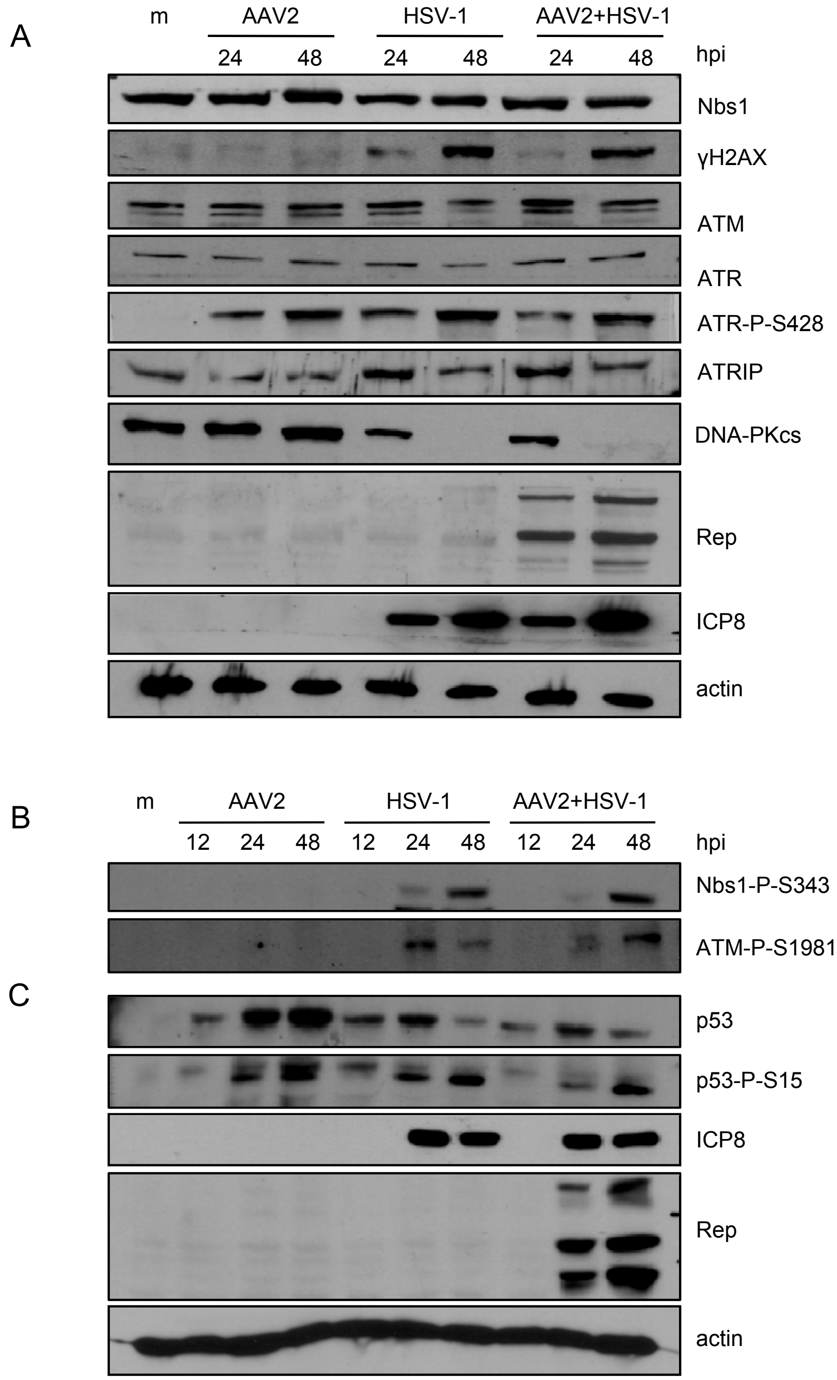

Vogel et al., Fig. 2

A

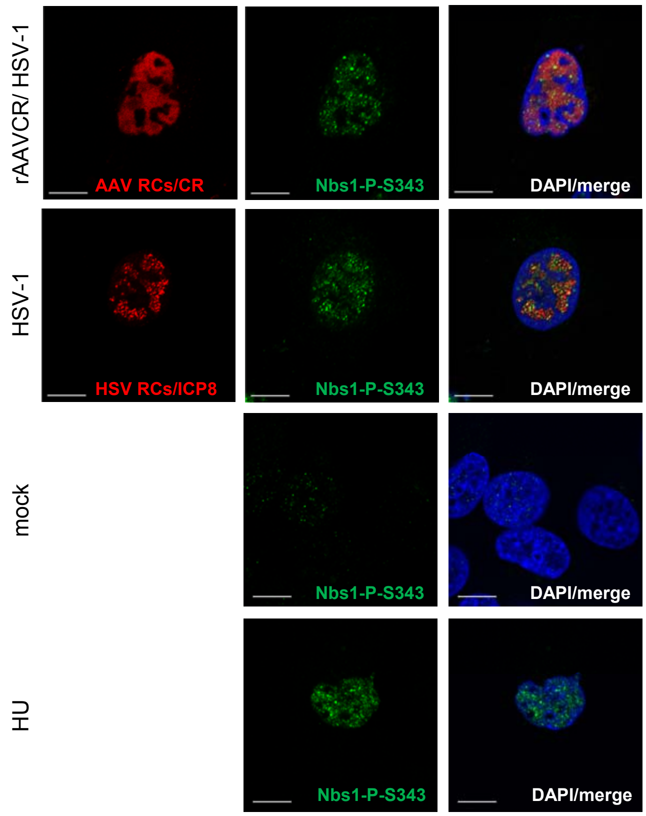

Vogel et al., Fig. 2

B

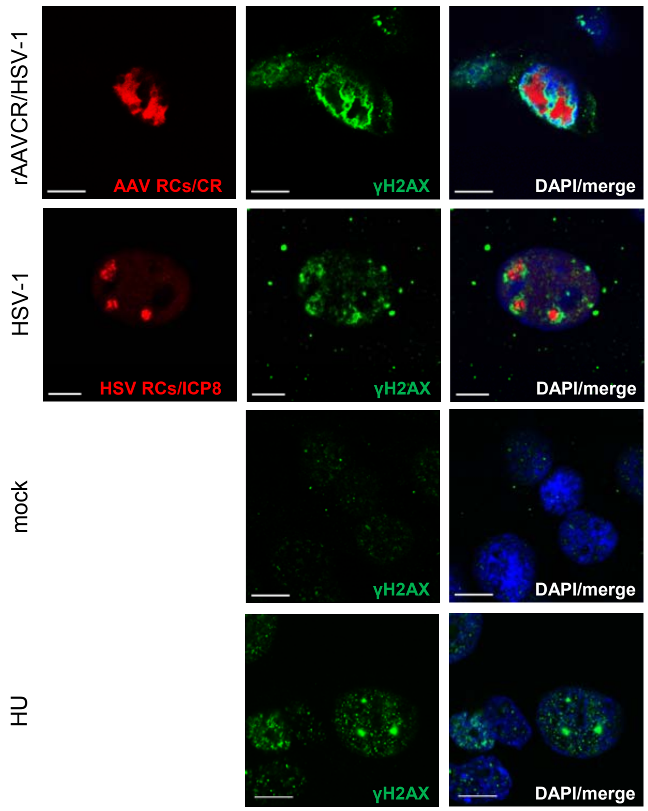

Vogel et al., Fig. 3

A

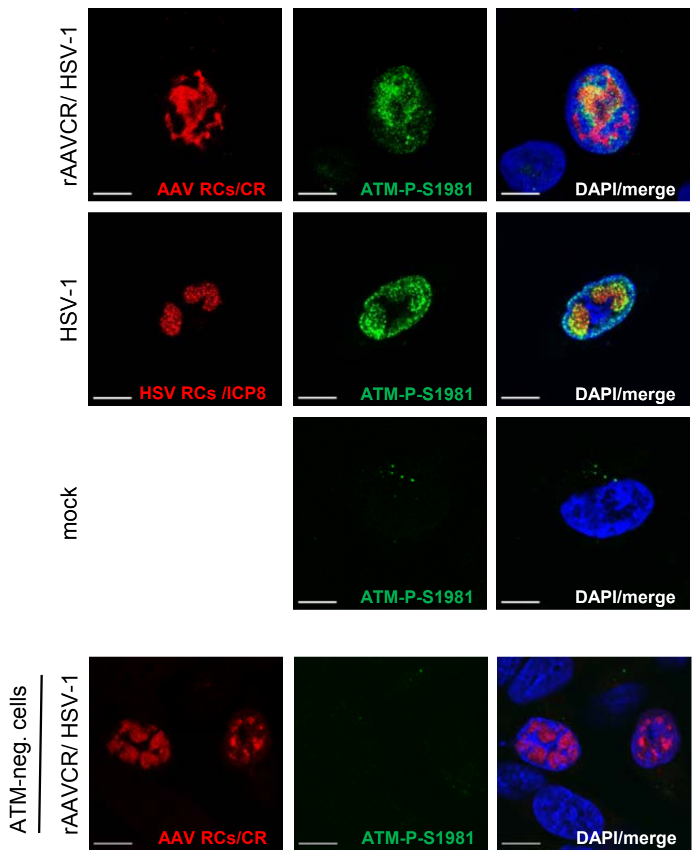

Vogel et al., Fig. 3

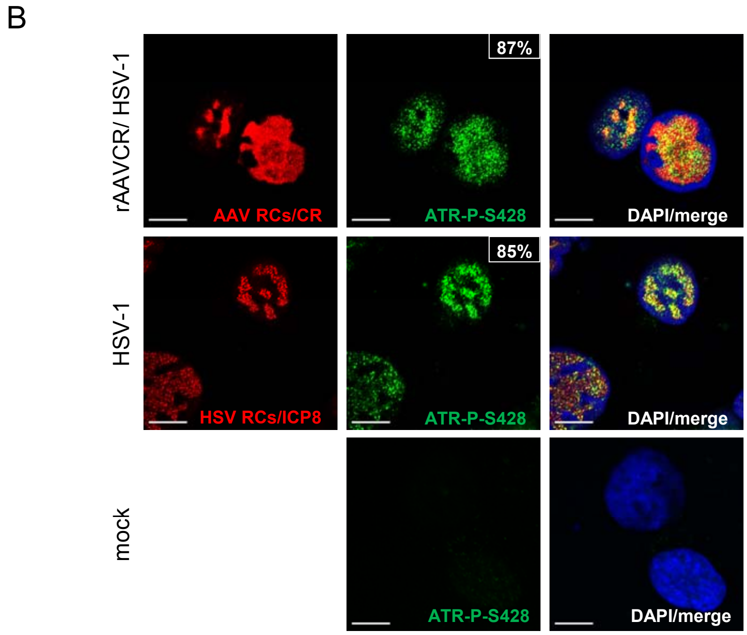

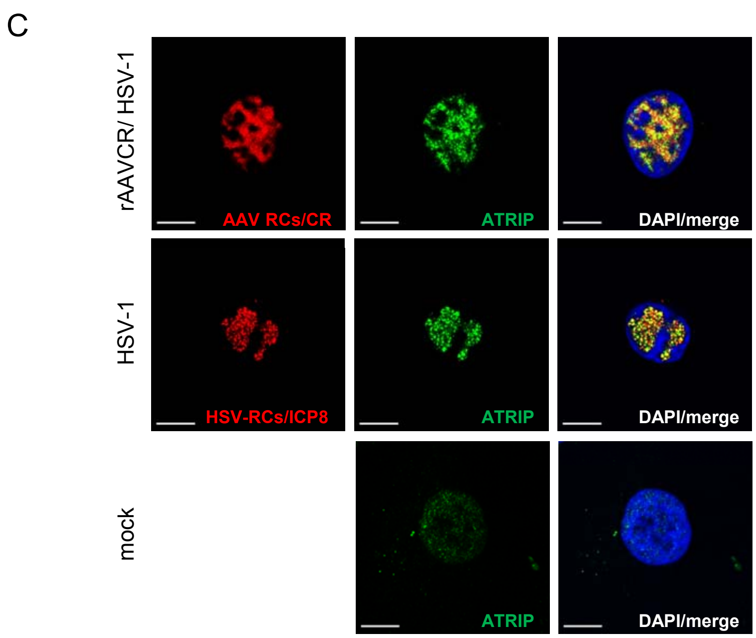

Vogel et al., Fig. 4

A

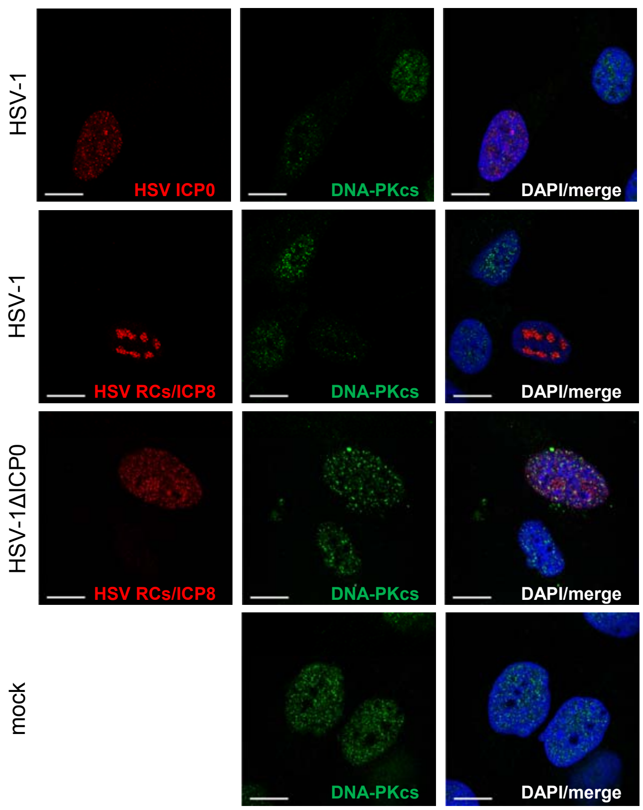

Vogel et al., Fig. 4

B

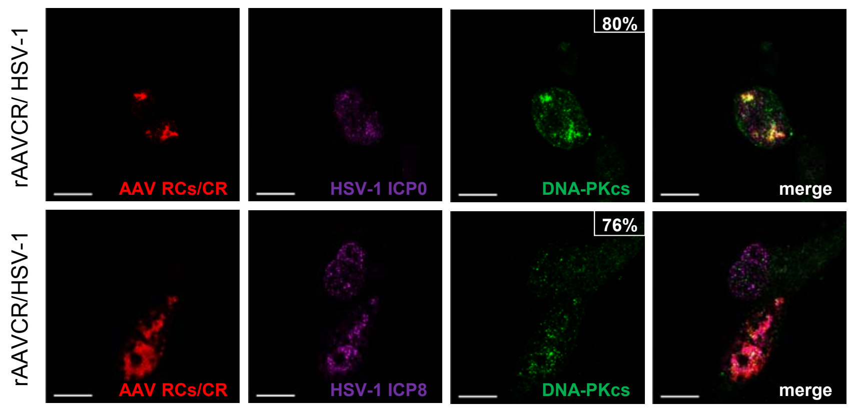

C

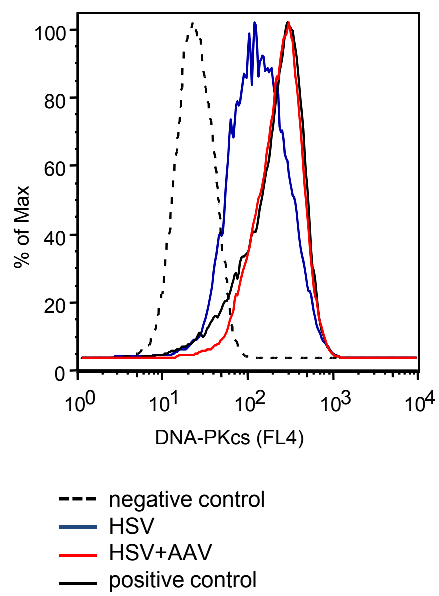

Vogel et al., Fig. 4

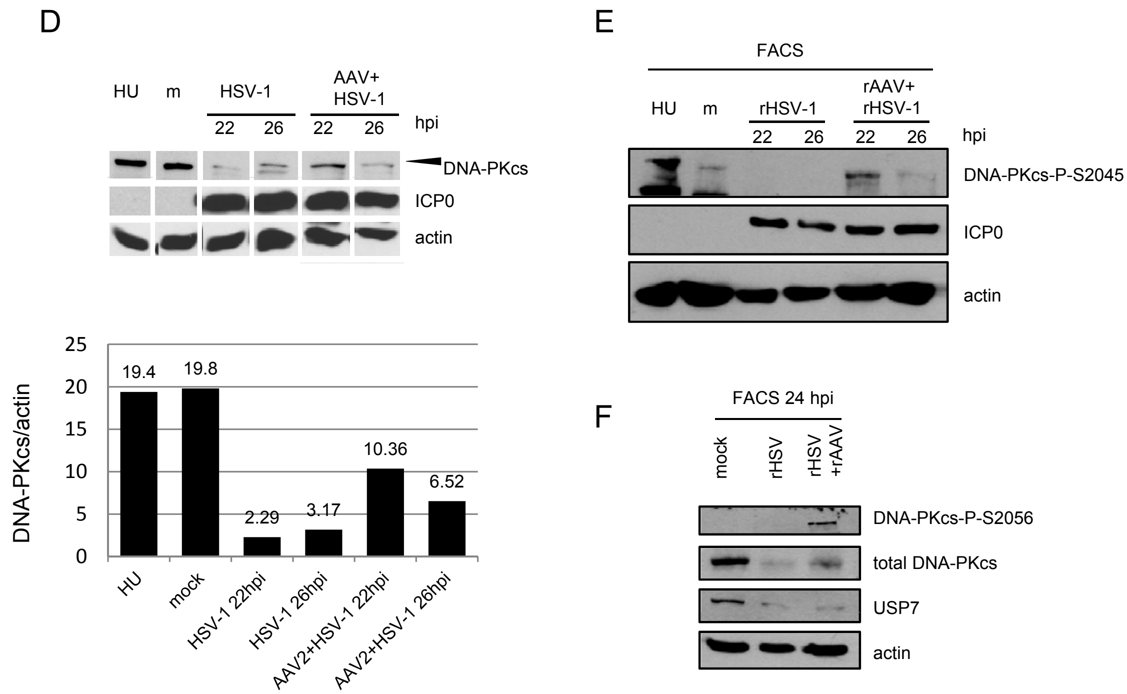

G

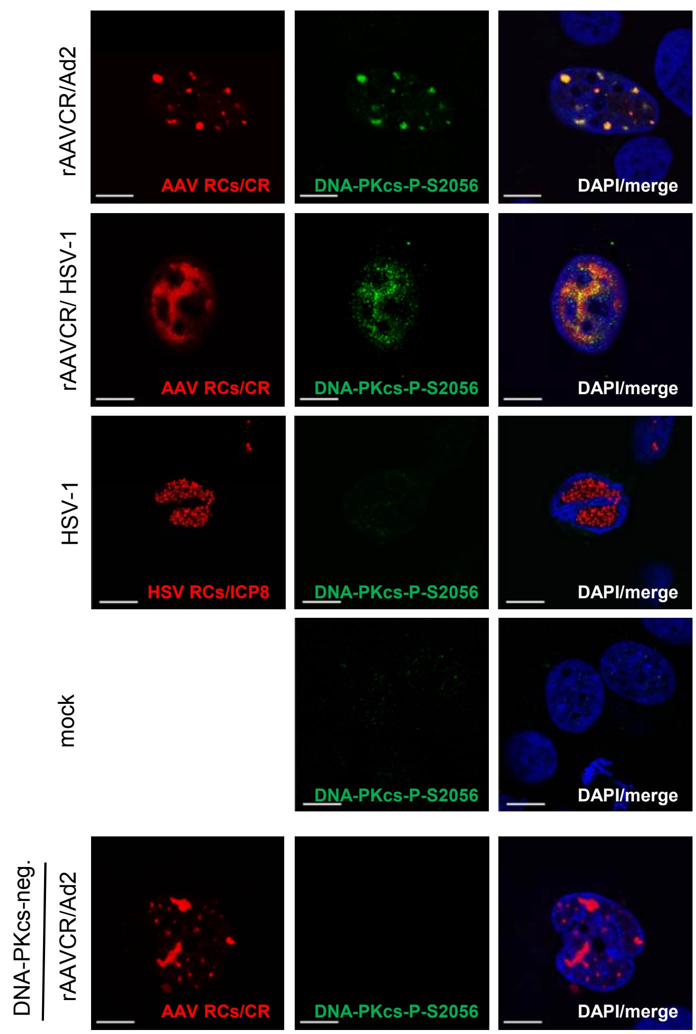
rAAVCR/Ad2
rAAVCR/ HSV-1
HSV-1
mock
DNA-PKcs-neg.
rAAVCR/Ad2
AAV RCs/CR
HSV RCs/ICP8
DNA-PKcs-P-S2056
DAPI/merge

Vogel et al., Fig. 5

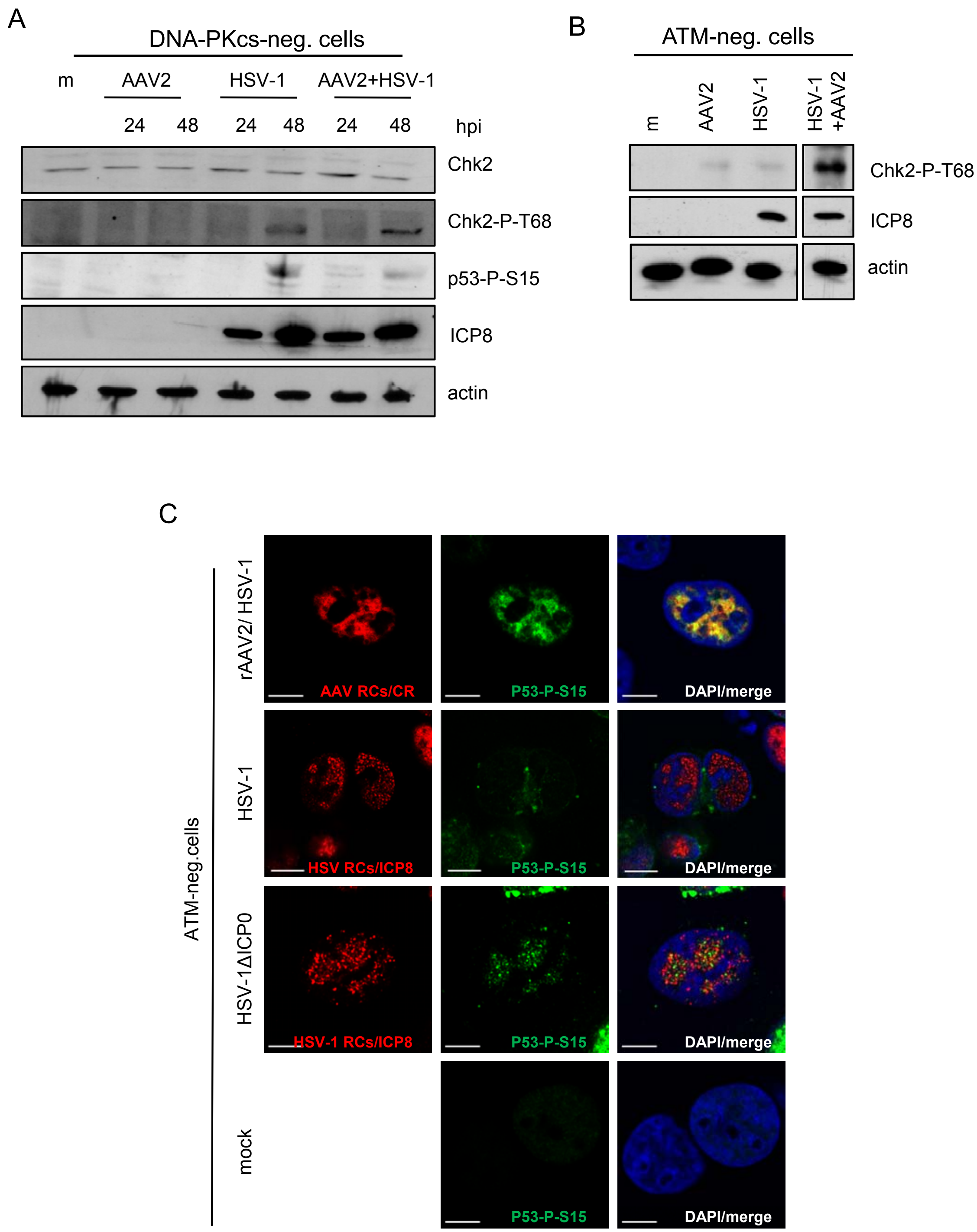

Vogel et al., Fig. 6

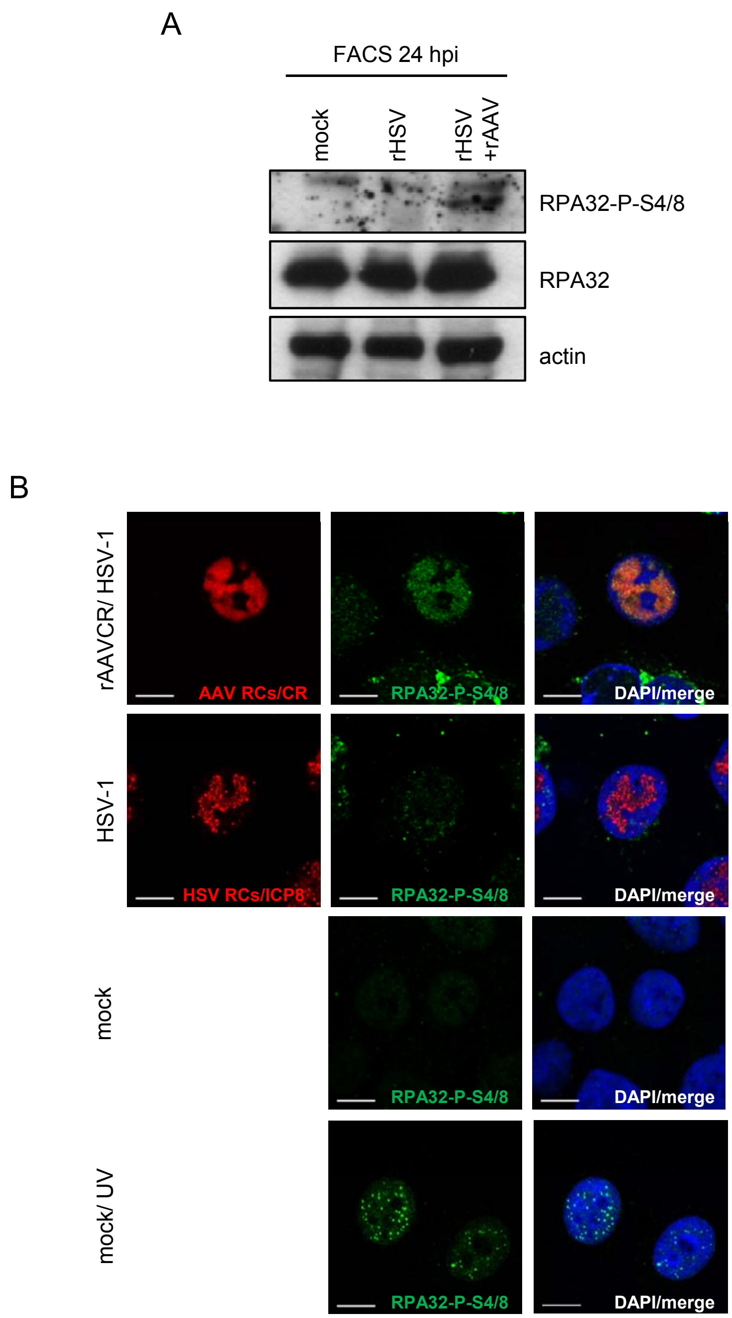

Vogel et al., Fig. 6